1

Bone and Other Skeletal Tissues

Ximena S. Villagran[1], Dirk J. Huisman[2], Susan M. Mentzer[3, 4, 5], Christopher E. Miller[3, 5] and Miranda M. Jans[6]

[1] *Museum of Archaeology and Ethnology, University of Sao Paulo, Brazil*
[2] *Cultural Heritage Agency of the Netherlands, Amersfoort, The Netherlands*
[3] *Institute for Archaeological Sciences, University of Tübingen, Tübingen, Germany*
[4] *School of Anthropology, University of Arizona, Tucson, USA*
[5] *Senckenberg Centre for Human Evolution and Paleoenvironment, University of Tübingen, Tübingen, Germany*
[6] *JOINT POW/MIA Accounting Command Central Identification Laboratory, JBPHH, HI, USA*

1.1 Introduction

Bone, teeth and other hard tissues derived from animals are a major artefact class of many archaeological sites. Fragments of these biological components can often constitute a significant portion of the coarse fraction of archaeological deposits (e.g., Schiegl *et al.* 2003; Dibble *et al.* 2009; Goldberg *et al.* 2012; Mentzer *et al.* 2015). The study of larger fragments of archaeological bone recovered during excavation is a central aspect of zooarchaeological and anthropological analysis. Geoarchaeologists encounter bones and teeth when conducting micromorphological analysis; however, the size of the bone fragments found during this type of study is often smaller than the size of those incorporated into more traditional zooarchaeological studies. Bones in thin sections of archaeological deposits therefore provide a different, but complementary, perspective on the archaeological remains of animals (Estévez *et al.* 2014). By studying these small-scale remains of bone in a thin section, micromorphologists can address a wide range of archaeological issues related to human behaviour, site formation processes, taphonomy and chemical diagenesis.

1.2 Micromorphology

1.2.1 Composition and Structure of Bone and Related Materials

Bone is a biological material that is produced by vertebrate animals. In living bodies, bone functions as both an organ and as a rigid skeleton that supports and contains soft tissues. Fresh bone is composed of inorganic calcium phosphates precipitated in an organic collagen matrix. More specifically, bones are generally composed of 20–30% collagen (protein) and 60–70% calcium phosphates (bone mineral), with the remaining <10% comprising a combination of other components such as complex sugars, lipids, carbonates, Mg, Na, trace elements and metal ions (White & Hannus 1983; Posner *et al.* 1984; Pate & Hutton 1988; Linse 1992; McCutcheon 1992; Currey 2002). The mineral component of bone is commonly referred to as: (i) hydroxylapatite or hydroxyapatite ($Ca_5(PO_4)_3(OH)$); (ii) bioapatite (a poorly crystalized calcium phosphate resembling hydroxylapatite); or (iii) carbonate hydroxylapatite ($Ca_5(PO_4CO_3)_3(OH)$) also known as dahllite (Pate & Hutton 1988; Linse 1992; McCutcheon 1992; White & Hannus, 1983; Stiner *et al.*, 1995; Karkanas *et al.* 2000; Hedges, 2002; Berna *et al.* 2004; Trueman *et al.* 2004; Smith *et al.* 2007). In reality, bone mineral is difficult to characterize. Mineralogical analyses reveal that pure hydroxylapatite is never actually found in bone or teeth, thus Weiner (2010) argues that this term should be reserved for geogenic, noncarbonated forms of apatite. Furthermore, the mineral dahllite is no longer recognized by the International Mineralogical Association. Therefore, despite the general inconsistencies found in the literature regarding bone mineral, the terms bioapatite, carbonate hydroxylapatite, or carbonate apatite are most appropriate.

The same combination of collagen and bioapatite occurs in mammal, bird, reptile and fish bones. The only exceptions are fish of the elasmobranch type (sharks, skates and rays), whose skeletons consist of cartilage containing a different type of collagen (type II) and no bioapatite (Szpak 2011).

Archaeological Soil and Sediment Micromorphology, First Edition. Edited by Cristiano Nicosia and Georges Stoops.

Besides bone, other hard biological tissues that can appear in the archaeological record are antler, teeth and keratin structures like horn and hair (of the aforementioned tissues, hair is the only nonskeletal one). **Antler** is a bony extension of the skulls of deer that has the same composition as bone (bioapatite, collagen, noncollagenous proteins and water – Currey 2002). **Teeth** are composed of three different hard biological materials: enamel, dentin and cementum. These materials have the same general composition as bone, but differ in the relative proportions of mineral to other components; enamel, dentin and cementum contain >95%, 75%, and 45% carbonate hydroxylapatite, respectively (Provenza & Seiber 1986; Weiner & Wagner 1998; Francillion-Viellot *et al.* 1990; Weiner 2010). **Horn** exists on animals from the Bovidae family (cattle, sheep, goat, etc.). It differs from bone in that it contains keratin (alpha-keratin, a fibrous protein also found in hair, nails, wool and claws) with minor amounts of bioapatite (Hashiguchi & Hashimoto 1995; Salamon 1999; Hashiguchi *et al.* 2001; O'Connor *et al.* 2015) or no crystalline phase at all (Tombolato *et al.* 2010). The **hair** fibre is made of hard keratin, water, lipids, pigment and trace elements (Wilson & Tobin 2010). Horn, hair and other keratinous tissues rarely survive in the archaeological record unless burial conditions impede biological activity (Wilson *et al.* 2007; Wilson & Tobin 2010; O'Connor *et al.* 2015).

In addition to having different compositions, hard biological tissues differ in their macroscopic structure. **Bones** can be divided into two different structures according to their porosity. Compact or cortical bone has low or null porosity. Spongy bone, also known as trabecular or cancellous bone, has high porosity. The boundary between both types is diffuse since compact and spongy represent a continuum (Weiner & Wagner 1998; Francillion-Viellot *et al.* 1990; Currey 2002; Weiner 2010). Spongy bone is frequently, though not exclusively, found in bone epiphysis or inside vertebrae, whereas dense compact bone is found in the shaft of long bones (bone diaphysis) or as part of flat bones (e.g., skull, scapula). **Antler** is composed of a combination of exterior compact bone and interior spongy bone (Goss 1983). **Teeth** exhibit a specific structural arrangement of enamel, dentin and cementum, from which only dentin is porous. The crown portion of the tooth is composed of enamel, which is thickest next to the crest of the cusp. The outer portion of the root is composed of cementum. The inner portions of the root and crown are composed of dentin (Carlson 1990). **Horns** contain fibrous keratinous tissue, and exhibit a gradient of porosity that is higher in the exterior and lower in the interior. They are attached to the skull by a short bony core made of spongy bone and covered with skin. Horns exhibit a hollow core when detached from the animal skull (Tombolato *et al.* 2010). The **hair** shaft is macroscopically smooth, but can have various shapes and thickness depending on the animal species and individual characteristics (Brunner & Coman 1974; Tridico *et al.* 2014).

1.2.2 Optical and Microstructural Properties of Bone and Other Skeletal Tissues

The optical properties of bone, teeth (including ivory), antler and keratin tissues (horn, hoof and hair) are summarized in Table 1.1. Different types of **bone** structures are visible in thin section. Compact and spongy bone can be easily recognized, despite the angle of the cut, due to the massive appearance that characterizes the former, and the large, closed-packed pores that characterize the latter (Figure 1.1a). At magnification, four fabric types of bone can be described. The basic component of bone material is the mineralized collagen fibril, which constitutes a combination of bioapatite crystals ($5 \times 25 \times 2–4\,nm^3$ plate-shaped crystals) and collagen fibrils (80–100 nm in diameter) (Lowenstam & Weiner 1989; Weiner 2010). The fibrils can be packed in four different ways (Currey 2002): woven bone (fibrils are randomly arranged) (Figure 1.1b); parallel-fibred bone (close-packed, parallel fibrils that have the same orientation); lamellar bone (fibrils are arranged in thin lamellae or sheets, like plywood, where each sheet differs in orientation of the fibrils) (Figure 1.1c); and fibrolamellar bone, which is a combination of woven and lamellar and/or parallel-fibred bone (Figure 1.1d, f). Different histological structures may be characterized by one or more type of fibril packing. For example, Haversian systems, which house blood vessels or nerves, consist of longitudinal vascular canals surrounded by concentric lamellar bone (Figure 1.1e). The appearance of bone in thin section depends both on the macrostructure, the arrangement of the fibrils and the angle at which the bone was cut during the preparation of the slide. For example, lamellar zones of compact bone show a pattern of intercalating dark and light bands in XPL (Figure 1.1f).

Both components of fibrils, the (quasicrystalline) collagen and the bioapatite, contribute to the appearance of bone under crossed polars. Both components, on their own, have low-order white to grey interference colours (Courty *et al.* 1989; Bromage *et al.* 2003); however, bone exhibits form birefringence, in which the birefringence of two materials influence each other. Both collagen and bioapatite are uniaxial, and their optical axes lie parallel to the axes of the collagen fibrils (Watson 1975; Wolman 1975; Stoops 2003). Collagen has a positive elongation sign, while bioapatite (and all apatite isomorphs), has a negative elongation sign (Bourne 1956; Watson 1975; Bromage *et al.* 2003). Although Courty *et al.* (1989) state that the mineral component is responsible for the

Table 1.1 Optical characteristics of bone, teeth, ivory, antler and keratin tissues (horn, hoof and hair). Note that pleochroism is absent in all the hard tissues.

Tissue	Colour (PPL)	Interference colour (XPL)	Autofluorescence (blue and UV light)	Figure	References
Bone	Light yellow	Low-order white to grey	Blue (UV), yellowish to green (blue light)	1.1a, 1.1f, 1.2a	Courty *et al.* 1989; Stoops 2003; Karkanas & Goldberg 2010
Antler	Light brown	Low-order white to grey	Yes	1.3a, b, c, d	Rolf & Enderle 1999; Skedros *et al.* 2014
Teeth					
Enamel	Light brown	Low-order white to grey	Blue light: no UV and red light: yes	1.3e, f	Schmidt & Keil 1971
Dentin	Pale brown and grey (with parallel fibers)	Grey and light orange (polarization cross visible in transversal sections of tooth)	Yes	1.3e, f, 1.4a, b, c, d	Schmidt & Keil 1971
Cementum	Pale brown	Low-order white with varying brightness	No	1.4a, b, c, d	Schmidt & Keil 1971
Ivory (fossil)	Brown	Low-order grey	Yes	1.4e, f	Su & Cui 1999; Heckel 2009; Virág 2012
Keratin tissues					
Horn	Light brown	Low-order grey	Yes	1.5a, b, c, d, e, f	Tombolato *et al.* 2010
Hoof	Yellowish brown	Low-order grey to high order	Yes	1.6a, b	Kasapi & Gosline 1997
Hair	Colourless to pale yellow	High order	Yes	1.6c, d, e, f	Wilson 2010; Wilson *et al.* 2010; Dejmal *et al.* 2014; Tridico *et al.* 2014

low-order interference colours of bone, Karkanas & Goldberg (2010), based on the work of Watson (1975), indicate that the interference colour of fresh bone is mostly due to collagen. Watson's conclusion is based on observations of bones that, after losing their collagen matrix, changed sign of elongation from positive (dominated by collagen) to negative (dominated by bioapatite). This change is also seen in the experimental heating of a fish vertebra at 100 °C and 500 °C (Figure 1.2).

In practice, the determination of elongation sign in bone must take into account the orientation and distribution of the collagen fibres, which may vary in different bones according to their biomechanical properties (Bromage *et al.* 2003). In the example given in Figure 1.2, if we consider the bioapatite and collagen fibres to be transversal to the medullary cavity, then there is a change from positive to negative elongation after heating. This fits Watson's proposal that collagen interference colour is dominant in fresh bone. However, if the fibrils are radially oriented, then the opposite situation is described (from negative to positive). Moreover, Bromage *et al.* (2003) state that the different interference colours seen in fresh bone are also determined by the orientation of its collagen, with transversal collagen fibres appearing white, longitudinal fibres appearing black and fibres with intermediate orientation showing different levels of grey under crosspolarizers.

The autofluorescence of bone can be attributed to the bioapatite component, although there is also a small contribution from collagen (Altermüller & Van Vliet-Lanoe 1990). Autofluorescence may be partly or completely lost as a result of decay or heating (see below) and its presence can be taken as indirect evidence of the degree of bone weathering (Hoke *et al.* 2011; Hollund 2013).

Antler has the same optical properties as bone with macrostructure comparable to that of long bones (an outer rim of compact bone and a core of spongy bone; Figure 1.3a–d; Table 1.1). **Teeth** can be identified by their overall morphology, as well as optical properties of the three components (dentin, enamel and cementum) (Table 1.1). In transversal cuts of the cusp, all vertebrate teeth show an outer layer of enamel, a core of dentin with radial orientation of fibrils, and polarization cross under XPL (see Figure 1.3e, f). The hollow centre of the tooth (pulp cavity) may be expressed as a void. In fossil or archaeological teeth, the dentine may have weaker

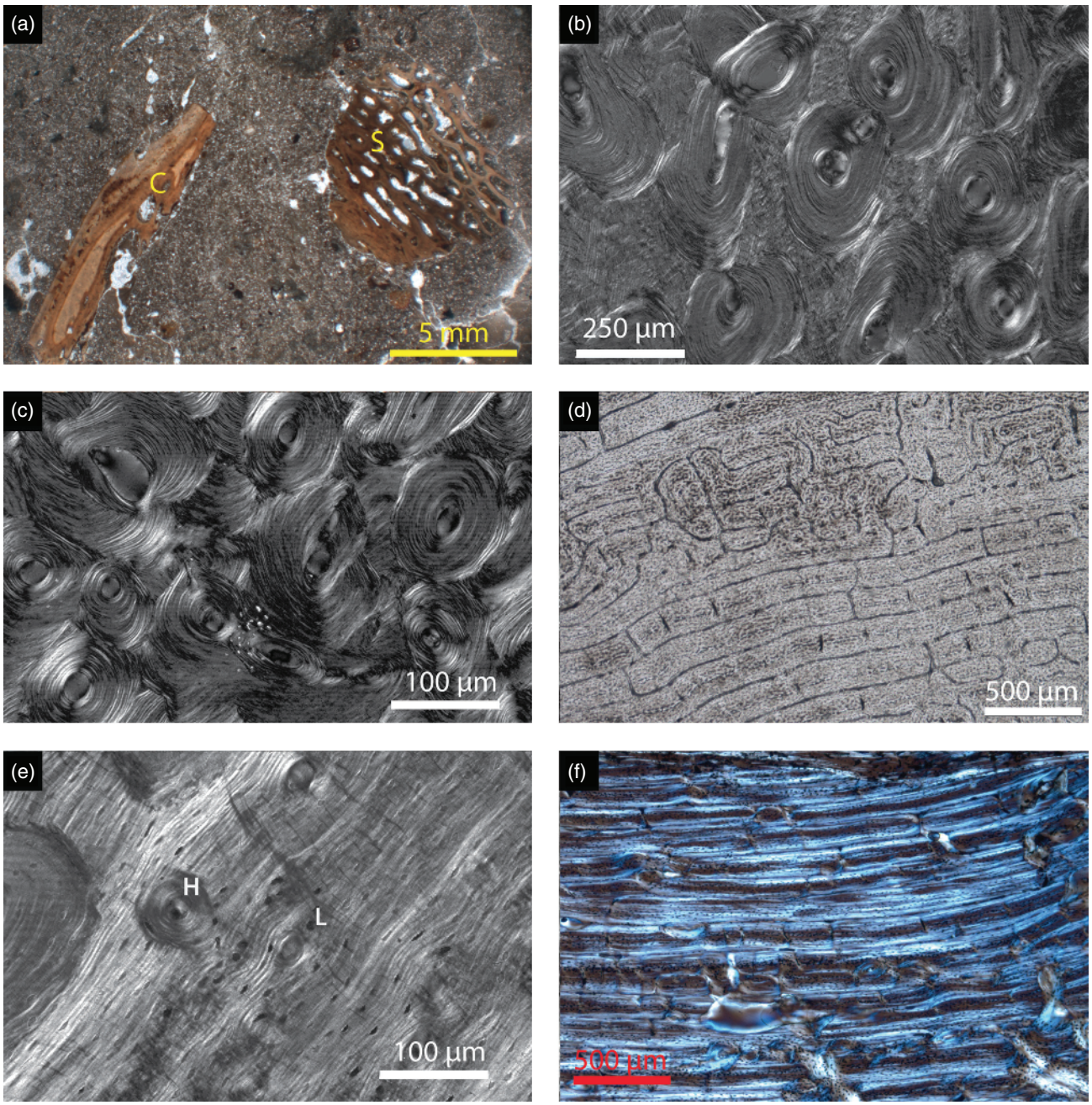

Figure 1.1 Examples of bone microstructures. (a) Fragments of spongy (S) and compact (C) bone fragments in a medieval deposit. PPL. (b) Microstructure of human bone (transversal cut) with osteons (circular canals with concentric lamellar bone) surrounded by woven bone. PPL. (c) Thin section of human bone (transversal cut) showing clear pattern of lamellar bone within and surrounding osteons. XPL. (d) Microstructure of fibrolamellar (plexiform) bone tissue (transversal cut) in deer bone section. PPL. (e) Haversian channel (H) formed in lamellar bone (L). (f) Fibrolamellar (plexiform) bone microstructure (transversal cut) of unknown mammal, probably ungulate. XPL.

birefringence or even appear completely isotropic (Schmidth & Keil 1971). Transverse cuts of the root exhibit outer layers of cementum and inner cores of dentin (Figure 1.4a–d). Longitudinal cuts may contain all three components. Depending on the cut, cementum may exhibit a scalloped morphology where it attaches to bone. Ivory, a specific type of dentin found in tusks of the order proboscidea, has distinct internal structures with parallel 'lines of Owen' (found in any dentin), and characteristic chevron-shaped 'Schreger patterns' that are only visible at low magnifications under PPL (see Su & Cui 1999; Heckel 2009; Virág 2012) (Figure 1.4e, f;

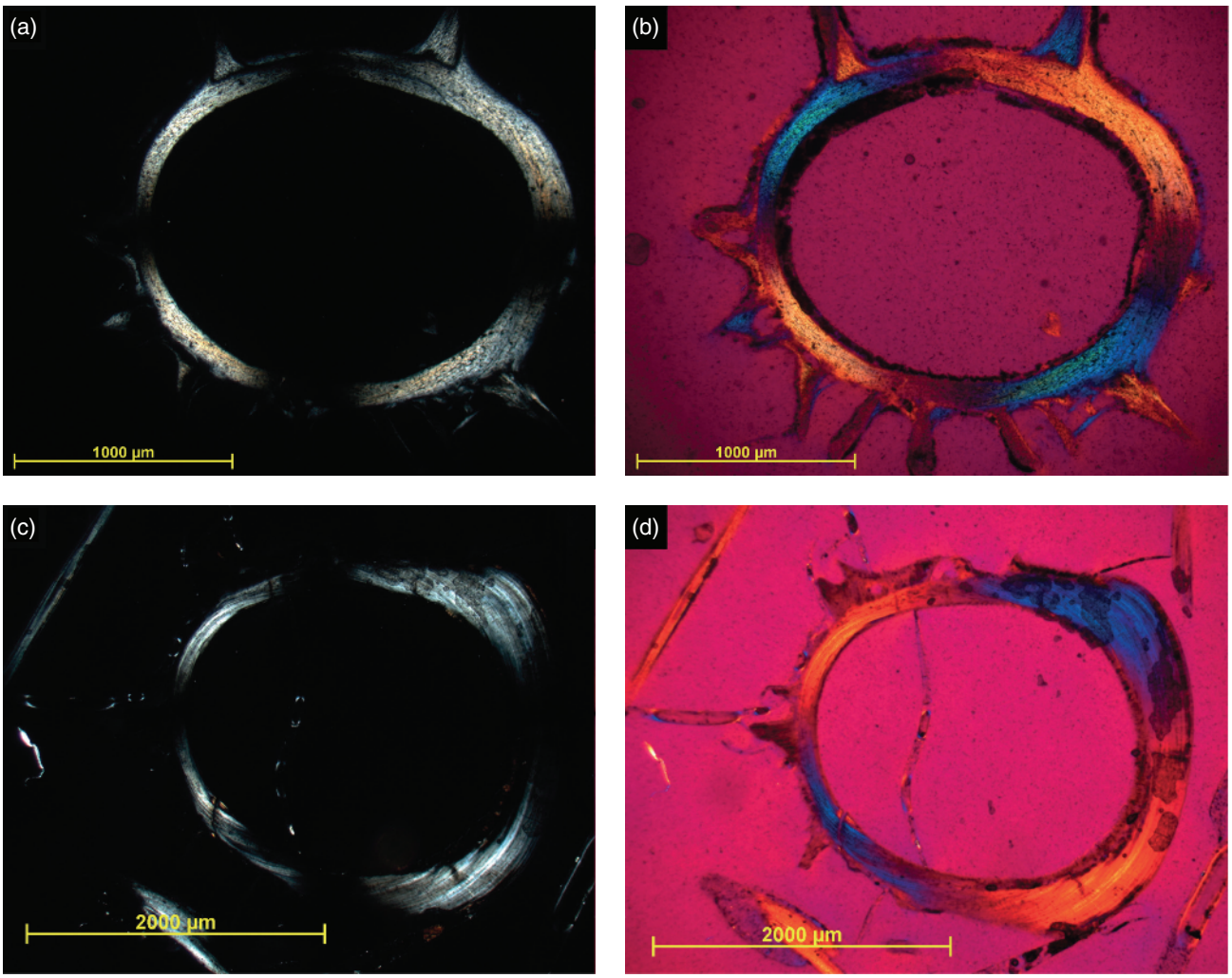

Figure 1.2 Thin sections from the experimental heating of fish vertebrae under oxidising conditions. (a) Transversal cut of vertebra heated at 100 °C in XPL. (b) Same as Figure 1.2a after insertion of gypsum plate, note positive elongation of bone, characteristic of collagen, when collagen fibres are transversally arranged. (c) Transversal cut of a vertebra heated at 500 °C in XPL, note lowering in interference colours. (d) Same as (c) after insertion of gypsum plate, note negative elongation, characteristic of apatite (see also Figure 1.5).

Table 1.1). These structures produce preferred cracking and delamination patterns that yield rectangular to equant fragments. The optical properties of horn, hoof and hair are those of keratin; however, they differ in morphology and microstructure (Table 1.1). The microstructure of **horn** is lamellar, with the lamellae extending along the length of the horn following the direction of growth (Tombolato *et al.* 2010). In transversal sections, the layering of the growth pattern is clearly visible, with darker banding parallel to the surface (PPL) and a speckled pattern in XPL (Figure 1.5a, c). The stacked bundles of lamellae can be seen in longitudinal sections of horn under PPL. Differences in the orientation of the lamellae result in a banded pattern with first to second-order interference colours (Figure 1.5b, d). The darker bands are autofluorescent under UV and blue light. However, longitudinal sections show little or no autofluorescence (Figure 1.5e, f). The keratinous wall of the horse **hoof** in thin section (Figure 1.6a, b) has a characteristic woven or cross-hatch fabric with regularly spaced channels visible under XPL. Its matrix is similar to that of compact bone, with circular lamellae of keratin around a hollow tubule (the medullary cavity) (Bertram & Gosline 1986; Kasapi & Gosline 1997; Tombolato *et al.* 2010). **Hair** (Figure 1.6c–f; see also Dejmal *et al.* 2014, Figure 10) has internal stratigraphy composed of an outer cuticle, an inner cortex and a central medulla (Brunner & Coman 1974; Wilson & Tobin 2010). Depending on the orientation of the hair, the rough morphology of the cortex may be visible. When affected by fungal tunnelling, the typical green fluorescence of hair turns red (Wilson *et al.* 2007; Wilson & Tobin 2010).

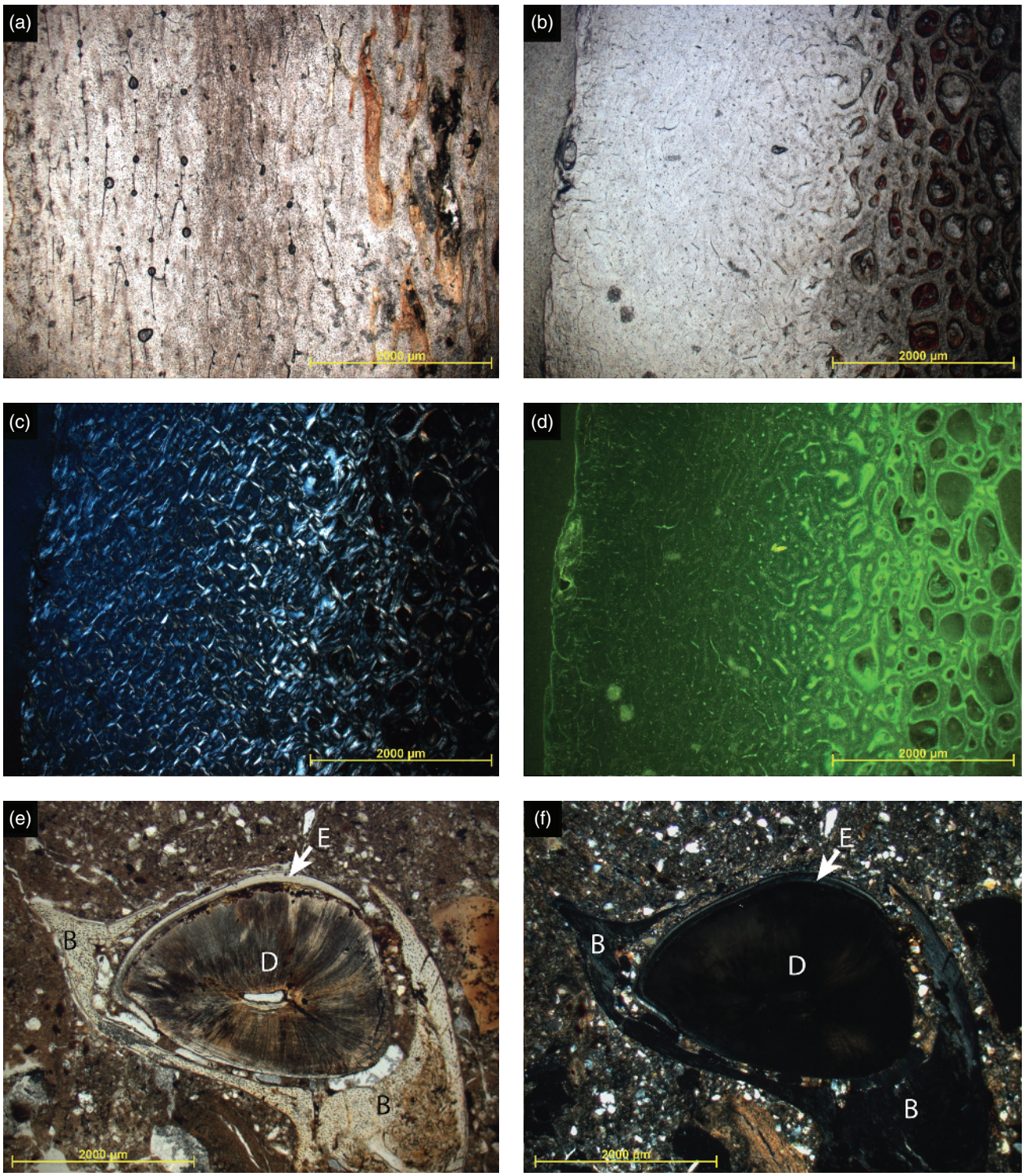

Figure 1.3 Microstructure of teeth, antler and ivory. (a) Longitudinal section of modern red deer antler, the spongy bone is seen as elongated structures (right of the image) next to the massive compact bone with vascular channels. PPL. (b), (c) and (d) Transversal section of red deer antler. Note transition from spongy (core) to compact bone (edges), as commonly seen in long bones. Spongy bone has stronger autofluorescence, possibly due to higher organic content. (b) PPL; (c) XPL; (d) BLF. (e) and (f) Transversal cut of a rodent tooth – still embedded in bone (B) from the skull or a jaw fragment – showing radial dentin (D) in the core and outer layer of enamel (E). Medieval occupation deposit (Achlum, The Netherlands). (e) PPL; (f) XPL.

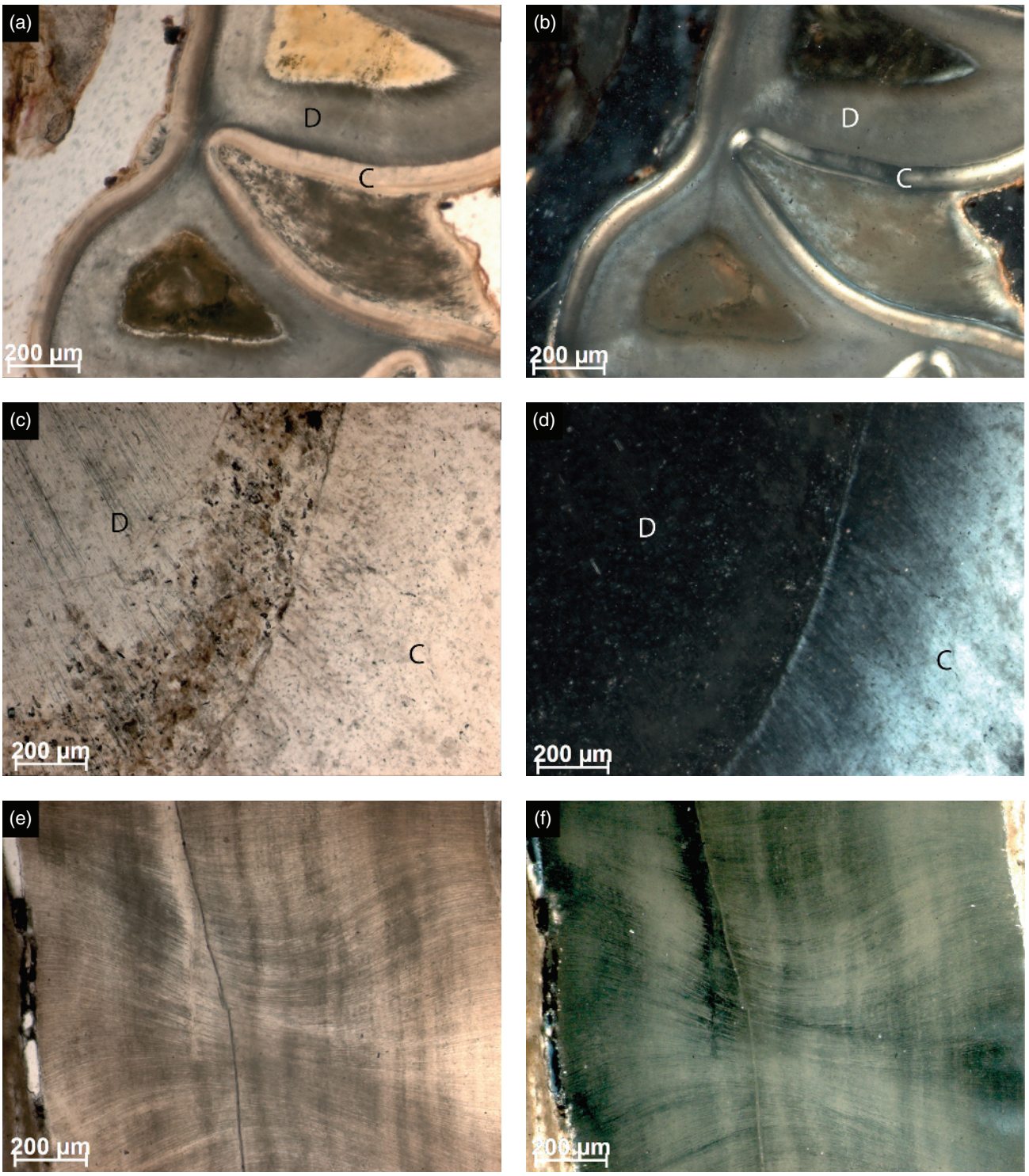

Figure 1.4 (a) and (b) Transversal cut through rodent molar, with dentin (D) and cementum (C). Note bone attached to the cementum: (a) PPL; (b) XPL. (c) and (d) Close-up of cementum (C) and dentin (D). (c) PPL; (d) XPL. (e) and (f) Fossil mammoth ivory: (e) PPL; (f) XPL.

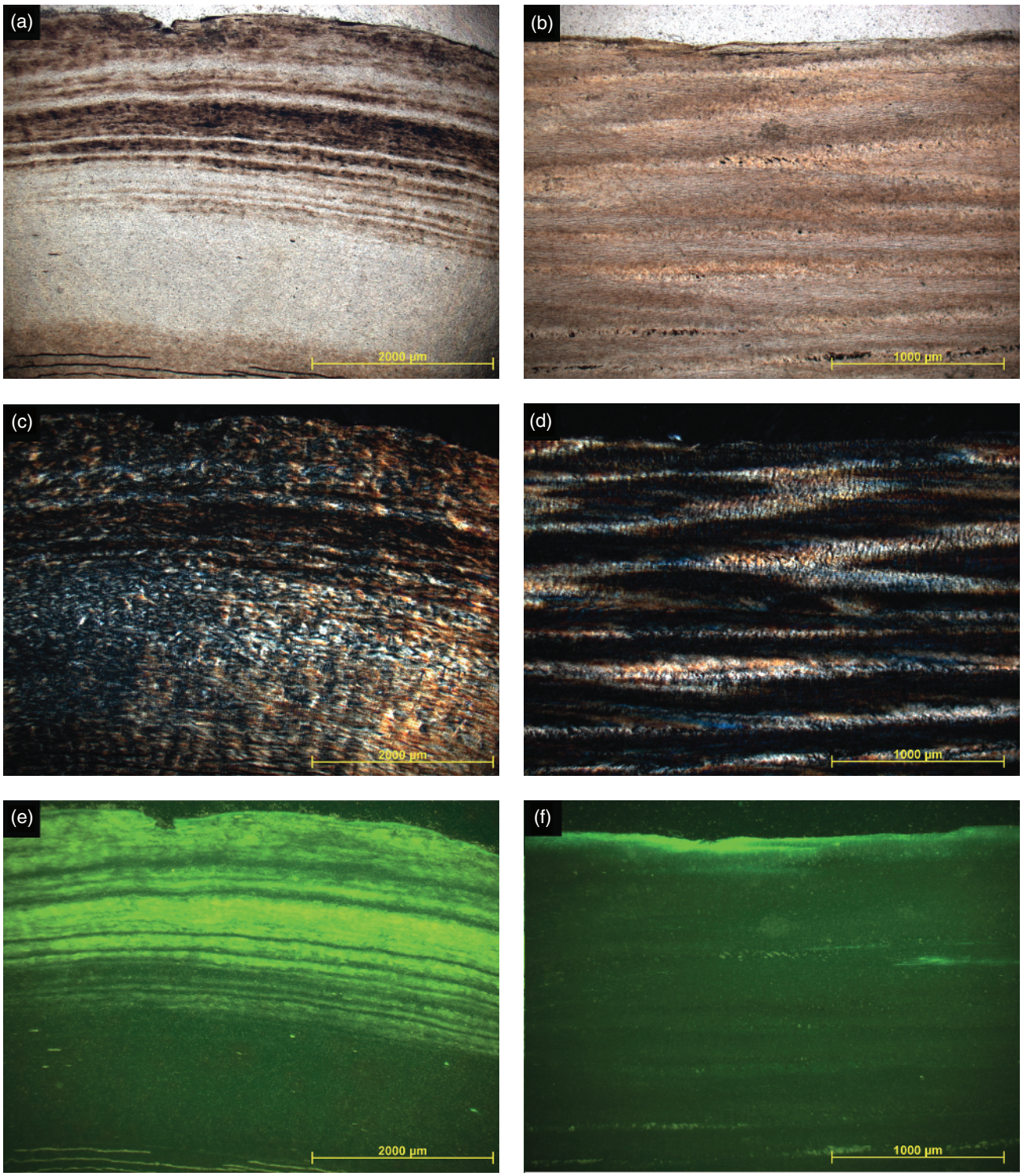

Figure 1.5 Horn and other keratinous tissue. Parts (a), (c) and (e) are transversal sections of modern cow horn: (a) PPL; (c) XPL; (e) BLF. Parts (b), (d) and (f) are longitudinal sections of the same horn: (b) PPL; (d): XPL; (f) BLF. Note growth lines in the transversal section and lamellae extending parallel to the length of the horn in the longitudinal section.

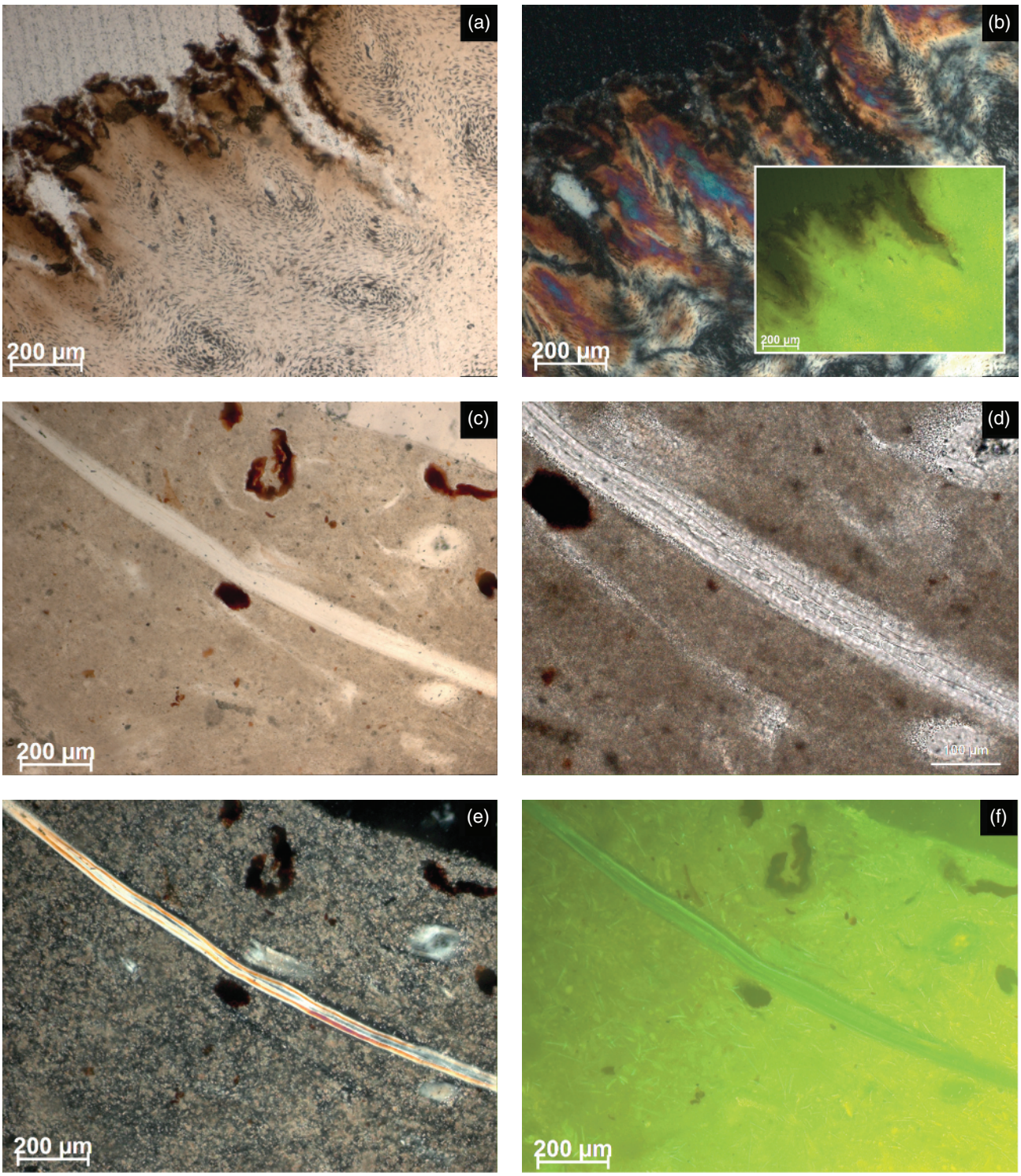

Figure 1.6 (a) and (b) Horse hoof. Inset in H shows BL image: (a) PPL; (b) XPL. (c), (d), (e) and (f) Hair in coprolite: (c) PPL; (d) PPL; (e) XPL; (f) BLF.

1.2.3 Identification of Bone Element and Animal Species from Thin Sections

In micromorphological samples it is rare to be able to identify the skeletal element – let alone determine the animal group or species – due to the small size of most bone fragments in thin section. For fragments of large bones it may be possible to distinguish between spongy and compact tissue in thin section (Figure 1.1a). In other situations, fortuitous orientations or sections may aid in identification of the element, especially if the element is whole or characteristic features are visible (e.g., the mandible pictured in Figure 1.3e, f).

Bones from humans and nonhuman mammals can be differentiated by morphology, DNA, proteins, or histological analysis. Plexiform bone is a specific type of compact / cortical fibrolamellar bone. Humans do not produce plexiform bone, so its presence in a large bone fragment may suggest that the source is nonhuman (Figure 1.1d). However, other primates and most small mammals also lack plexiform bone, which in the case of small fragments can prevent a straightforward identification. Furthermore, plexiform bone can be removed from the bones of large animals by weathering. In these ambiguous cases, measurements of certain histological structures (e.g., the diameters of Haversian systems) in oriented sections are necessary (Hillier & Bell 2007) (Figure 1.1c, d, f).

Although identification of most animal groups or species is difficult in micromorphological samples, an exception is seen in certain bones that are clearly diagnostic of fishes. Fish scales can be easily distinguished in thin section by their denticulate surface (Figure 1.7a, b) and fish vertebrae are unmistakably identified by their cross-shaped or rounded morphology (Figure 1.7c, d). Different bones that comprise the fin rays also show particular shapes that allow for their identification in thin section. The proximal portion of fin rays is made of thin, elongated bones with thicker and rounded extremities (Figure 1.7e), while the lepidotrichia (the distal portion of the fin) is made of successive paired small bones, which exhibit shapes similar to parenthesis (Figure 1.7f) (Francillion-Vielot *et al.* 1990). In addition, recent studies demonstrate that micro CT (microcomputed tomography) scanning of micromorphological blocks provides three-dimensional information about bone fragments and may facilitate species determination when samples contain small bones (Huisman *et al.* 2014b; Ngan-Tillard & Huisman 2017, this book).

1.3 Taphonomy of Bone

Taphonomic processes that impact bones include combustion and heating, biological activity, mechanical fracturing and chemical weathering. Identification of the traces of these processes in bones visible in thin section can aid in reconstructing site formation processes, including syndepositional human activities such as burning and trampling and disturbance of sites by animals. Other processes can be indicative of past environments and burial settings. Micromorphology can also be integrated to the solution of taphonomic problems raised by zooarchaeological analyses (the microtaphonomic approach, *sensu* Estévez *et al.* 2014).

1.3.1 Combustion and Heating of Bone

Burning can occur incidentally, for example when bones are located underneath a hearth, or intentionally when they are burnt for fuel (Schiegl *et al.* 2003), used to manage specific properties of the fire (Théry-Parisot 2002), or subjects of site-maintenance practices (Clark & Ligouis 2010). Only the organic constituents (i.e., fat and collagen) of bone truly burns; however, the mineral fraction of bone also becomes altered by heat, providing a means for identifying and tracking heating in the past. Other types of heating, such as roasting, baking and boiling, produce characteristic compositional and structural changes, including loss of collagen at low temperatures (Roberts *et al.* 2002).

According to Ellingham *et al.* (2015) bone can undergo four stages of transformation related to burning or incineration: (i) dehydration, (ii) decomposition, (iii) inversion and (iv) fusion. Several experimental studies have shown that bones progress through predictable stages of colour alteration corresponding to degree of heating (e.g., Shipman *et al.* 1984; Stiner *et al.* 1995; Bennett 1999; Hanson & Cain 2007). These stages include: fresh, unburnt bone, which appears ivory or tan in colour; partially carbonized or charred bone, which can appear brown or reddish; fully carbonized or charred bone, which appears black; and white calcined bone, in which all organic material and moisture is removed. Despite these numerous studies, some controversy remains as to what temperature corresponds to which colour change (Ellingham *et al.* 2015). Some researchers note that the initiation of the different stages of colour change vary between bones derived from mammals, birds and fish (Nicholson 1993), whereas others point out the amount of flesh and fat covering a bone can also significantly influence the onset of colour changes due to heating (Symes *et al.* 2008).

Table 1.2 summarizes experimental data produced from modern bones burnt or heated at a variety of temperatures. Two sets of burning experiments were conducted on ungulate and fish bones, which were then processed into thin sections (see also Figures 1.8, 1.9, 1.10). Petrographic observations of these bone samples are included; however, it is important to stress that many

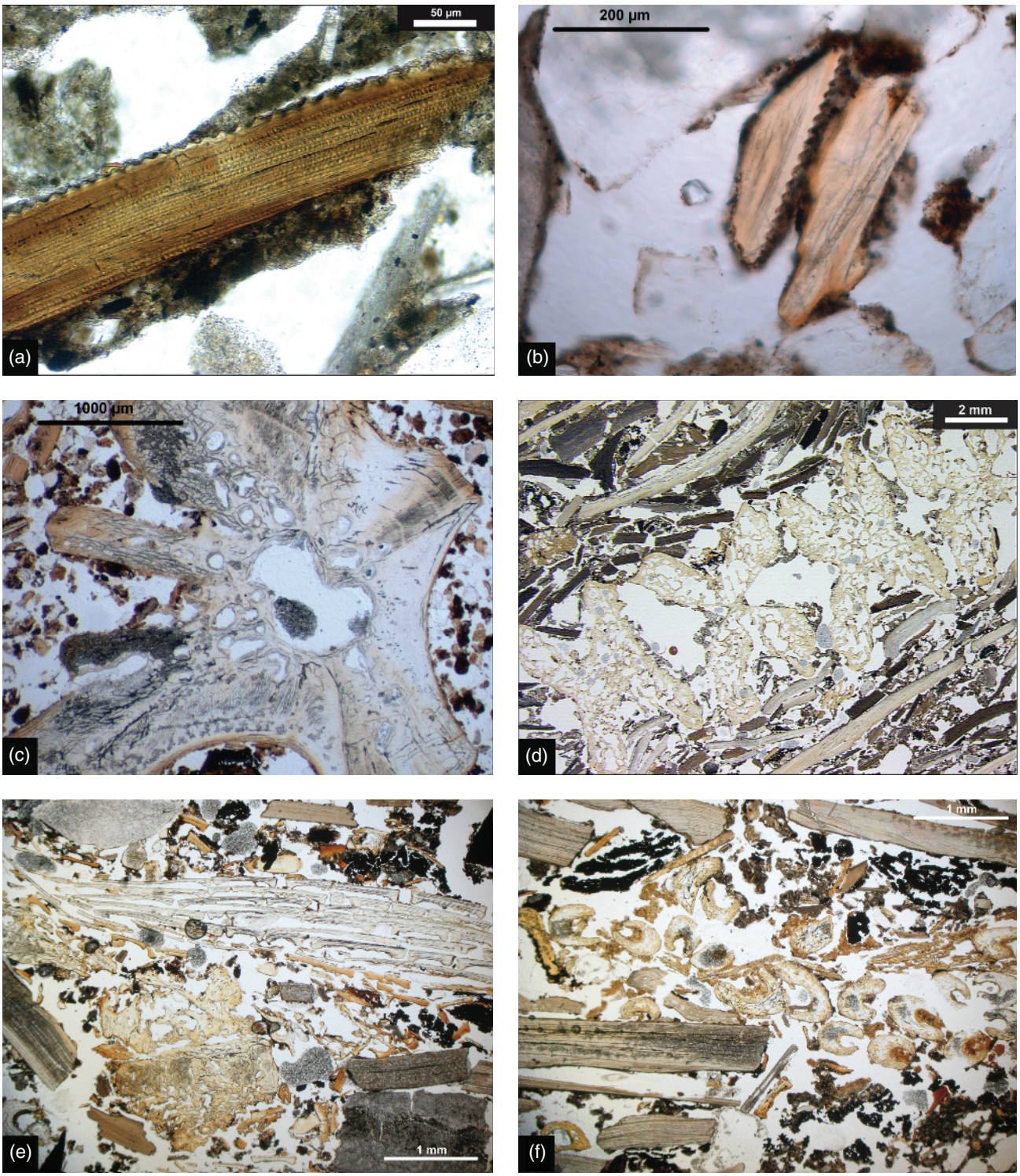

Figure 1.7 Fish bones. (a) Fish scale with typical denticulated edge. Caipora shell mound (c. 7440–6110 cal. yr BP, Santa Catarina, Brazil – see Estevez *et al.* 2014; Villagran 2014). PPL. (b) Small fragment of fish scale. Same site as Figure 1.5a. (c) Section of a fish vertebra, Santa Marta 8 fish mound (c. 1550 cal. yr BP, Santa Catarina, Brazil – see Villagran 2014. PPL. (d) Section of four articulated fish vertebrae, Cubatão shell mound (c. 3000 BP, Santa Catarina, Brazil). PPL. (e) Articulated bones from a fin ray (fr). Sernambetiba shell mound (c. 2000 BP, Rio de Janeiro, Brazil). PPL. (f) Dispersed bones from fin ray lepidotrichia (fr). Sernambetiba shell mound (Rio de Janeiro, Brazil). PPL.

Table 1.2 Micromorphological characteristics of experimentally heated bone in thin section. n.d. = no data. Thin sections of pig and cow bones: the unburnt samples (bone and teeth) are from the personal reference collection of P. Goldberg; the sample heated at 100 °C is a boiled reindeer bone collected by L. Binford from an ethnographic context. Thin sections of fish bones courtesy of M. Canti.

Temperature in °C (heated to +/– 10 °C)	Micromorphological characteristics of *pig and cow bones* in thin section (temperatures held for 45 minutes)	Micromorphological characteristics of *fish bones* in thin section (temperatures held for 30 minutes)
Unburnt	Colourless (transparent) in PPL. Strong low-order interference colours (white, grey, black). Strong fluorescence under blue and UV light.	n.d.
100	Colourless (transparent) in PPL. Strong low-order interference colours (white, grey, black), strongly contrasting. Weak to moderate fluorescence under blue light; moderate under UV light.	Colourless (transparent) to light grey in PPL. Strong birefringence in XPL. Low order interference colours.
200	Colourless (transparent) in PPL. Strong low-order interference colours (white, grey, black), strongly contrasting. Moderate fluorescence under blue light; moderate to strong under UV light.	As above.
300	Light to medium yellow, ranging to dark reddish brown in PPL. Weak abnormal olive brown, to grey brown interference colours. Moderate to strong fluorescence under blue and UV light, except in areas with reddish brown colour in PPL.	Light to medium yellow in PPL. Weak to moderate grey to white interference colours.
400	Dark reddish brown to black (opaque) in PPL. Weak interference colours (reddish in areas that are reddish brown in PPL). Absent to very weak fluorescence under blue light; absent to weak fluorescence under UV light.	Reddish brown to black (opaque) in PPL. Weak abnormal interference colours, reddish in areas that are reddish brown in PPL.
500	Pale brown to black (opaque) in PPL. Weak abnormal olive brown to dark blue-grey interference colours. Weak to moderate fluorescence under blue light in areas that are brown in PPL, absent to moderate fluorescence under UV light.	Pale brown in PPL. Moderate blue-grey interference colours.
600	As above.	Colourless (transparent) to brown in PPL. Moderate blue interference colours.
700	Pale brown in PPL. Weak to moderate low order greys. Interference colours are with low contrast. Absent to very weak fluorescence in blue and UV light.	As above.
800	Brown to brownish grey in PPL, with visible internal fissures. Moderate to strong bluish grey interference colours with an overall milky cast (accentuated by the substage condenser). Small crystal aggregates with higher interference colours are visible within the bone tissue. Absent to weak fluorescence in blue and UV light.	As above.
900	Brown to brownish grey in PPL, with visible internal fissures. Strong white to grey interference colours with an overall milky cast (accentuated by the substage condenser). Absent to very weak fluorescence in blue and UV light.	Pale brown in PPL. Weak to moderate low order grey to blue-grey interference colours.
1000	As above	As above.
1100	n.d	Opaque in PPL. Moderate low-order grey interference colours with an overall milky cast.
1200	n.d.	Translucent in PPL. Weak to moderate low order grey interference colours.

of the observed features, such as colour in PPL and interference colours can be impacted by a variety of sample preparation parameters and taphonomic conditions. These include the angle at which the bone is cut, slide thickness, microscope light source and use of the substage condenser, as well as chemical and biological alteration (see section 1.3.3).

The data presented in Table 1.2 are broadly consistent with published observations from archaeological samples. Many researchers have noted the distinctive milky

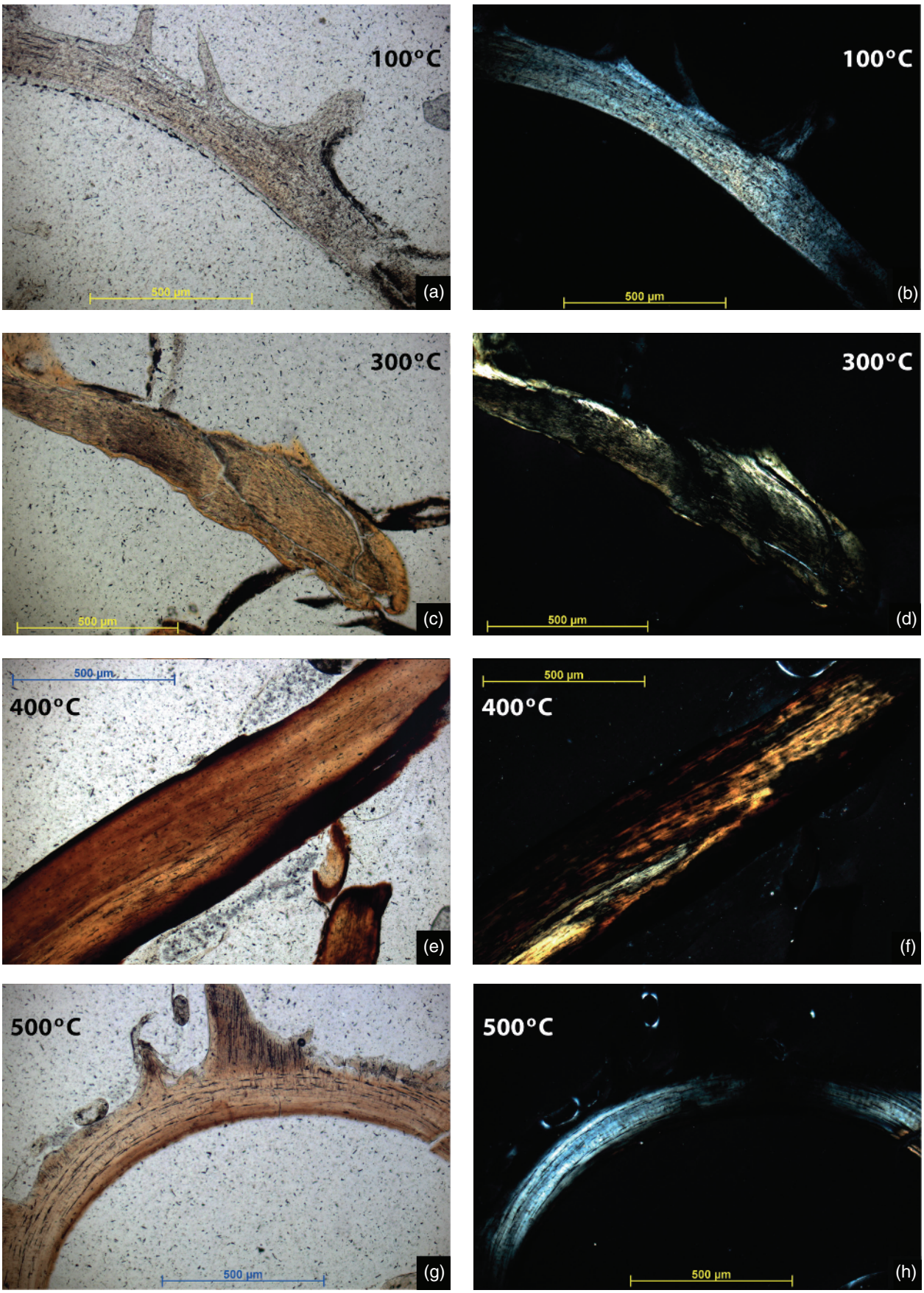

Figure 1.8 (a)–(h) Thin sections of herring bone heated from 100 °C to 500 °C under oxidising conditions. Images in PPL (left) and XPL (right). From 100 to 400 °C, the colour of bone changes from light grey to yellowish orange and reddish brown to black (PPL). Interference colours go from first-order yellow and white between 100 and 300 °C. Second-order reddish interference colours appear at 400 °C (XPL). Thin sections courtesy of M. Canti.

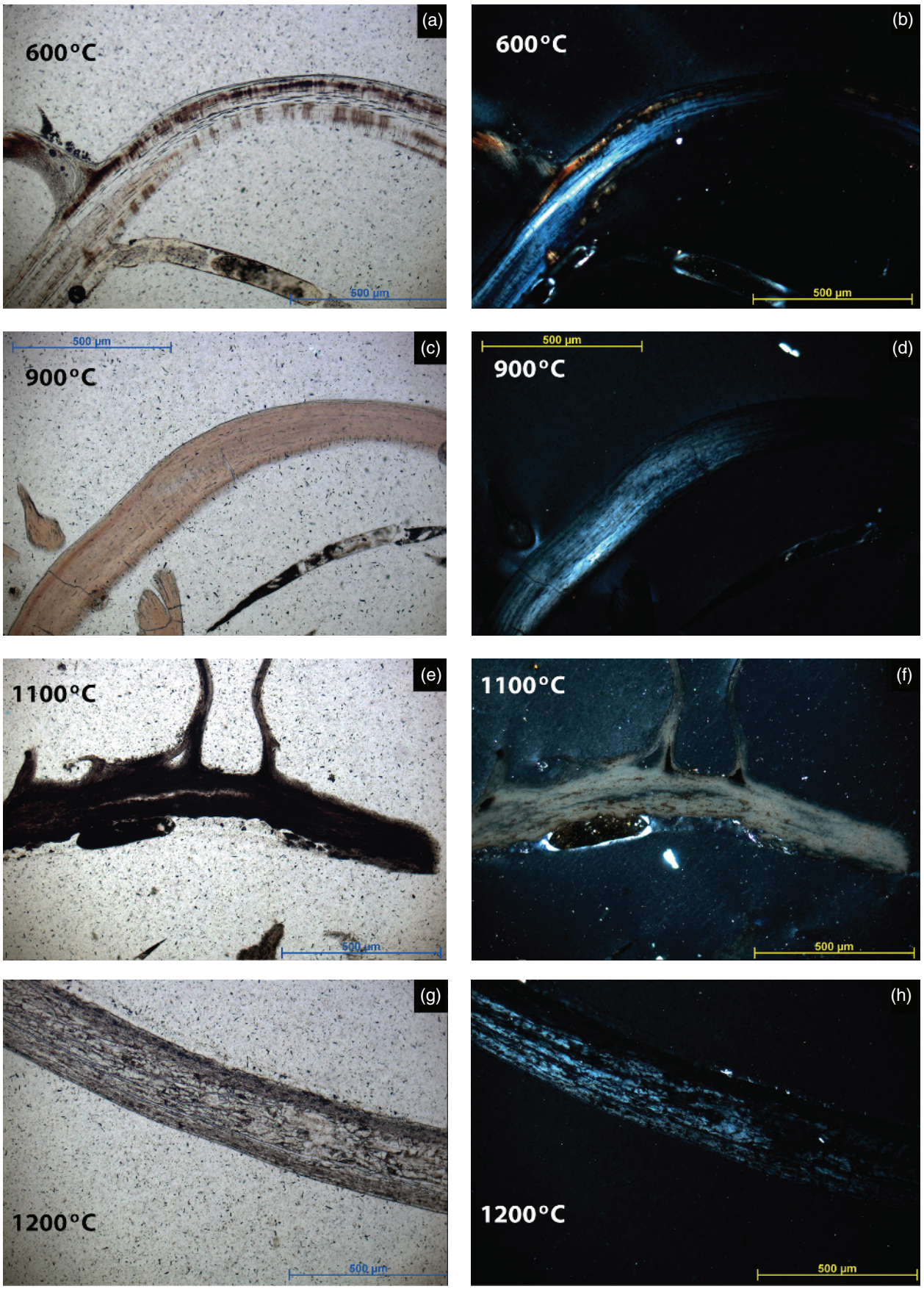

Figure 1.9 (a)–(h) Thin sections of herring bone heated from 600 °C to 1200 °C under oxidising conditions. Between 500 °C (Figure 1.8) and 900 °C bones turn pale brown with blue-grey and blue interference colours (XPL). Bone heated to 1100 °C is opaque (PPL) with cloudy or milky appearance (XPL). At 1200 °C, the bone is again pale brown (PPL) and shows lower order white and grey interference colours (XPL). Thin sections courtesy of M. Canti.

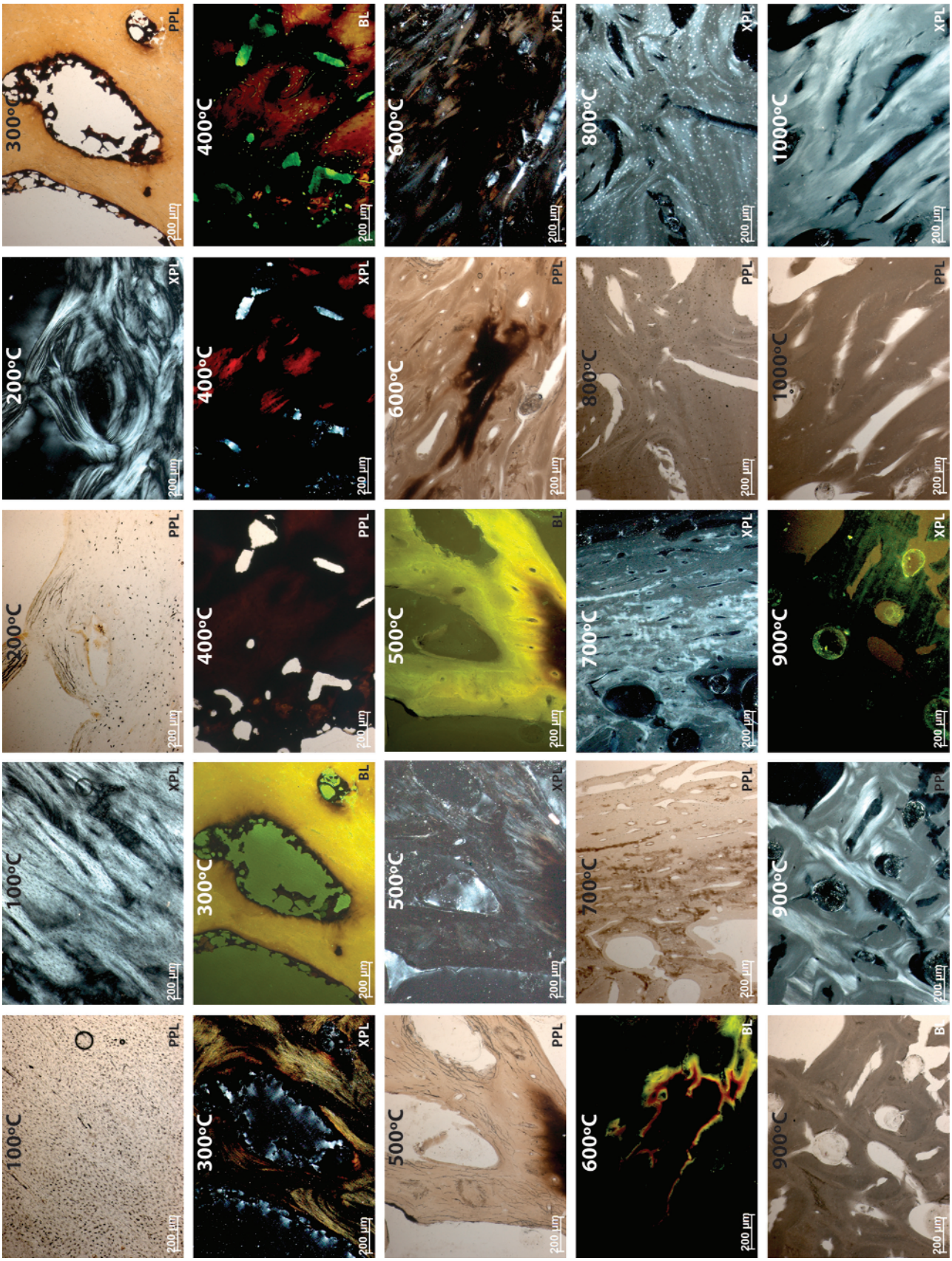

Figure 1.10 Thin sections of ungulate bone heated from 100 °C to 1000 °C under oxidising conditions. At 100 °C sample corresponds to boiled reindeer bone, at 300–600 °C and 800–900 °C samples come from heated cow bones, and at 700 °C and 1000 °C samples are pig bones. No major difference is seen between bones heated at 100 °C and 200 °C. At 300 °C bones turn light to medium yellow (PPL) with olive brown to grey brown interference colours (XPL) and moderate to strong fluorescence (BLF). At 400 °C bones turn dark reddish brown (PPL) with red interference colours with opaque areas (XPL). Colour changes to pale brown (PPL) between 500 and 700 °C. Interference colours are olive brown to dark blue-grey between 500 and 600 °C, turning to low order grey at 700 °C (XPL). Fluorescence is now weak to moderate (BLF). Between 800 and 1000 °C bones are brown to brownish grey (PPL) with strong birefringence (XPL) and low order interference colours from bluish grey to grey with milky cast typical of calcined bone. Fluorescence is weak to absent (BLF).

cast to the birefringence of calcined bone under XPL (e.g., Schiegl *et al.* 2003; Mentzer *et al.* 2015). Schiegl *et al.* (2003), in a study of a burnt bone deposit, suggested that bones exhibiting darker, opaque colours of brown and black in PPL are likely carbonized. They also argue that bones that appear almost colourless in PPL, but with first-order interference colours in XPL, suggest a lack of collagen and recrystallization of apatite or calcination.

Several studies have reported a decrease or loss of autofluorescence under UV light as a common sign of heating in bones due to loss of collagen (Courty *et al.* 1989; Schiegl *et al.* 2003; Karkanas *et al.* 2007) (see Figure 1.11a). The results from experimental heating of pig and cow bone described in Table 1.2 and Figure 1.10 are broadly consistent with this observation. Autofluorescence under ultraviolet (UV) and blue light decreases significantly above 500 °C. In contrast, the heated fish bones described in Table 1.2 retained autofluorescence throughout the complete experimental temperature range. This difference may be due to the duration of heating (30 min). For instance, Thompson *et al.* (2009) found that, although molecular changes began to occur in bones heated for 15 , they recommended 45 min of heating for future experiments.

When heating occurs in nonoxygenated environments (e.g., bones buried in the soil underneath a fire) bones turn black macroscopically (Stiner *et al.* 1995). In thin sections, this may be seen as a coat of sootlike charred organic material on the surface of the heat-altered bone (Figure 1.11b). In larger bones, lack of oxygen during heating may result in charring of fat or marrow or in the accumulation of soot inside the bone. This results in the formation of opaque black precipitates in the bone microstructure that mask the optical properties of the bone mass (Figure 1.11c).

Despite general trends in presence and absence of certain optical properties with temperature, these properties alone are not the best approach to identifying burned bone in thin section. Mineral staining can mimic colour change in PPL caused by low temperature heating. Similarly, small fragments of charred bone can resemble other charred organic remains, particularly a black amorphous substance identified as 'fat-derived char' (Berna & Goldberg 2008; Goldberg *et al.* 2009) (Figure 1.11d). This material is produced from burning of flesh, bone and / or animal fat and has been identified in diverse archaeological contexts (Goldberg *et al.* 2012; Miller *et al.* 2013; Villagran *et al.* 2013). It exhibits numerous vesicles with small fissures or cracks radiating from the walls (Figure 31.6e in Mallol *et al.* 2017, this book) which, when the fragments are sufficiently large, should allow for distinction between it and charred bone, or 'bone char'. The appearance of pale brown or orange fragments of bone that exhibit variations in the interference colour and fluorescence can be due either to low temperature heating or to collagen decay after microbial alteration or chemical dissolution (Schoeninger *et al.* 1989; Trueman & Martill 2002; Trueman *et al.* 2004). The lack of equifinality in the optical characteristics of burnt bone and bone modified by other processes requires the use of other microanalytical techniques to determine if bones found in thin section have been subjected to heating. The application of FTIR, FTIR microscopy, XRD, histomorphometry, measurements of crystallite size and organic petrography to loose samples and thin sections has been shown to be helpful in distinguishing between bones subjected to heating and those subjected to other alteration processes (Shahack-Gross *et al.* 1997; Karkanas *et al.* 2007; Piga *et al.* 2008; Dibble *et al.* 2009; Thompson *et al.* 2009; Clark & Ligouis 2010; Goldberg & Berna 2010; Lebon *et al.* 2010; Reiche 2010; Squires *et al.* 2011; Berna *et al.* 2012; Ellingham *et al.* 2015).

1.3.2 Mechanical Fracturing of Bone

There are numerous causes of bone fragmentation: intentional human practices, such as butchery and burning; unintentional trampling; and syn- and post-depositional physical processes, including wetting and drying, freezing and thawing, formation of secondary salt crystals and overburden pressures. The effects of these processes have been widely investigated through taphonomic studies; however, most cannot be distinguished using micromorphology alone. Some processes, described below, can be clearly recognized in thin section, whereas others can be identified from aspects of the sedimentary matrix. Therefore micromorphology of fragmented bone can provide a valuable data set that complements more traditional zooarchaeological studies.

Trampling of bones, whether by humans or animals, can cause distinctive fractures that are readily identifiable in thin section. Experimental work conducted by Miller *et al.* (2009) determined that trampling can cause *in situ* snapping of bone, leading to articulated, accommodating fragments of slightly displaced bone (Figure 1.11e). Bones with significant pore space, such as spongy bone, will often exhibit lower degrees of accommodation and appear 'crushed'. Fracture patterning similar to that found in the experiments has been reported in archaeological thin sections and attributed to human trampling (Dibble *et al.* 2009; Goldberg *et al.* 2009). Similar types of *in situ* fracturing could be caused by pressure related to sediment overburden, an interpretation offered for fractured bone at the site of Tönchesberg (Conard 1992). However, as far as we are aware, no micromorphological studies of bones fractured by sediment overburden have been conducted. Trampling can also cause horizontal displacement of

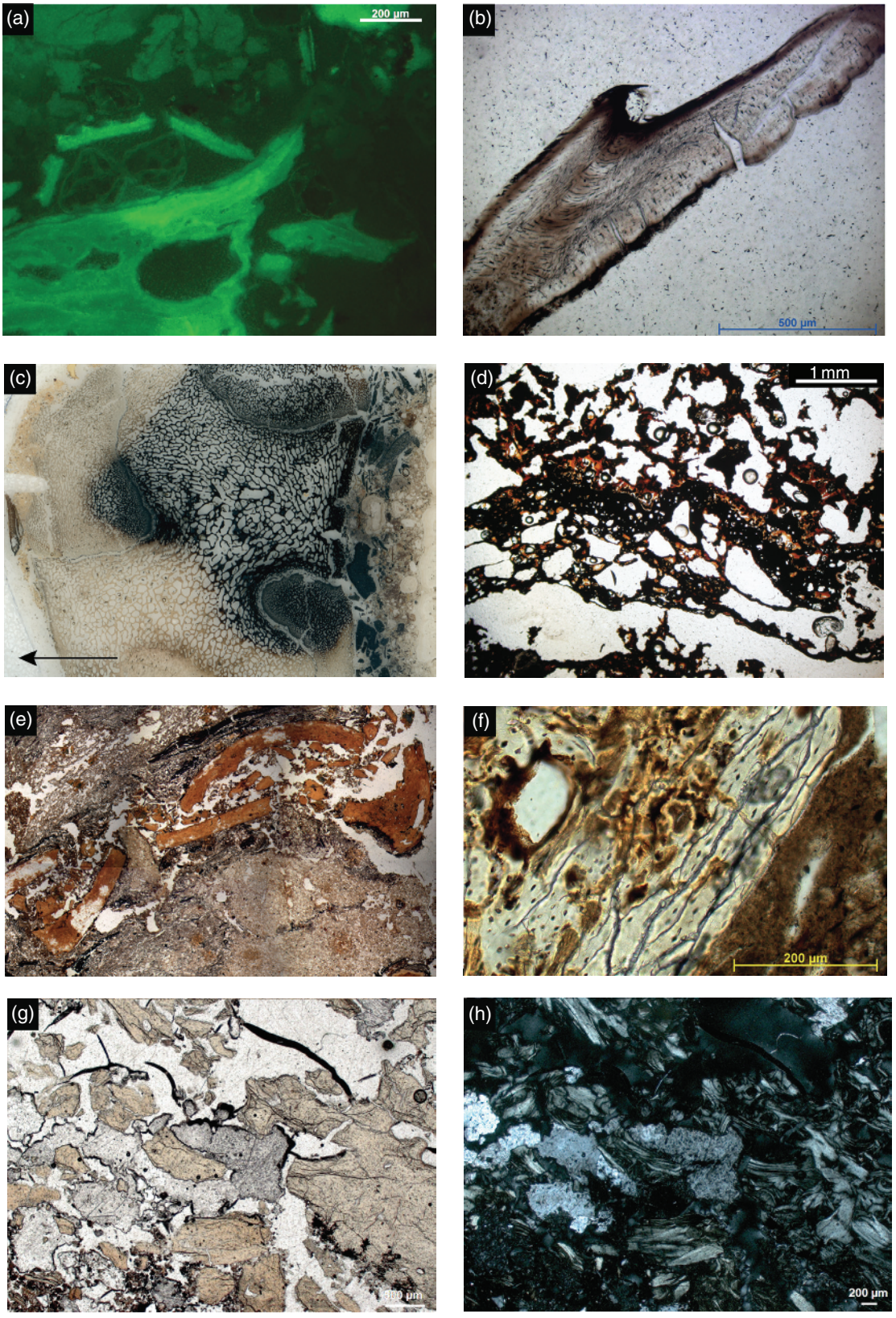

Figure 1.11 Various effects of heating on bone (a–d). (a) Burnt and fresh bones from the Santa Marta 8 fish midden (c. 1550 cal. years BP, Santa Catarina State, Brazil). Note the auto-fluorescence of fresh bone fragments compared to the weak to absent fluorescent burned fragments. BLF. (b) Herring bone experimentally heated to 700 °C in absence of oxygen. Note the dark edges due to the presence of soot. PPL. (c) Thin section scan showing a fragment of horse bone experimentally burnt for 8 hours in an open hearth with average temperatures below 300 °C. Note the dark colours on the inside of the bone due to charring. Image width 68 mm. Image courtesy: C. Mallol. (d) Fat-derived char from a combustion feature at the seventeenth–eighteenth century site of Sealer 4, Livingston Island (Antarctica – see Villagran *et al.* 2013). Note its characteristic homogeneous black colour and vesicular shape that can easily be mistaken of charred spongeous bone (see Figure 1.8c). PPL. Bone cracking and fragmentation (e–h). (e) The breakage pattern, with accommodating fragments in articulated position or with little displacement indicates *in situ* breakage, probably due to trampling. Iron Age midden-like deposit (Oosterbeintum, the Netherlands). PPL. (f) Localized zone of cracking in surface of rodent skull (see Figure 1.3a, b). This pattern occurs only in the outer surface layers of the bone, and is probably due to preburial exposure. PPL. (g) and (h) Secondary minerals forming in-between bone fragment and breaking it apart. Middle Stone Age deposits in Sibudu (South Africa): (g) PPL; (h) XPL.

materials, including fragments of bone. In this case, the bone fragments do not exhibit articulation or accommodation but they appear subrounded and incorporated within deposits composed of a heterogenous mix of various components (Goldberg *et al.* 2009; Miller *et al.* 2013).

Bone exposed on the surface or subsurface for extended periods can be affected physically by repeated drying and wetting and / or freeze-thaw cycles. Such cycles can result in physical damage characterized by patterns of fine fissures, as seen in Figure 1.11f. Schiegl *et al.* (2003) and Miller (2015) report a deposit composed almost exclusively of sand-sized fragments of bone at the cave site of Hohle Fels; the bone fragments appear subrounded and exhibited laminated coatings of calcareous silt, which the researchers interpret as having formed by cryoturbation.

Moisture containing dissolved ions within archaeological deposits can collect within pre-existing fissures and pores in bones where, upon evaporation, crystals can form. As the crystals grow they exert pressure on the surrounding bone, which leads to fracturing and fragmentation (Figure 1.11g, h). This process is most common in sites that are relatively dry, and have alkaline burial conditions with sources for dissolved ions that preferentially form crystals (Behrensmeyer 1978). Crystal-induced fragmentation of bone due to gypsum formation has been reported from the rockshelter sites of Sibudu (Goldberg *et al.* 2009) and Diepkloof (Miller *et al.* 2013) in South Africa. A similar process has been observed with secondary calcite at Qesem (Karkanas *et al.* 2007) and Obi-Rakhmat (Mallol *et al.* 2009).

1.3.3 Alteration through Biological Processes

Biological activity can contribute to the mechanical and chemical transformation of bone in archaeological sites. The type and scale of impacts depend on the organism responsible. For example, fungi and plant roots produce characteristic chemical weathering patterns on bone surfaces (Behrensmeyer 1978). Aside from mechanical fragmentation due to root activity, the effects of plants on bone are difficult to identify in thin section. In contrast, other nonhuman biological taphonomic agents are more recognizable. These include macrofauna, mesofauna and microbes.

1.3.3.1 Macro- and Mesofaunal Decay

Carnivores and omnivores scavenge and consume fresh and ancient bones from surface and subsurface deposits in archaeological sites. These activities are evidenced by macroscopic damage as well as bone fragments visible in coprolites (see Brönniman *et al.* 2017, this book). Macphail & Goldberg (2010) note that leaching of bones during their passage through the digestive channels of dogs, humans and birds results in loss of both birefringence and autofluorescence. However, this may not always happen. For example, bones in dog or human coprolites from the site of Swifterbant S4 (Huisman *et al.* 2009) do not show evidence of dissolution. Alteration by soil mesofauna can sometimes be documented in thin section. For example, in temperate environments, earthworms and insects may consume bone fragments and excrete them in their faecal pellets (see for example Figure 1.12a). In tropical settings, decay of bones by termites is a well-known phenomenon (e.g., Huchet *et al.* 2011; Backwell *et al.* 2012).

1.3.3.2 Microbiological Decay

Bone collagen is rich in nitrogen, which makes it a desirable potential resource for microflora and fauna. Furthermore, if bone is buried as part of a complete body, putrefaction and decay of soft tissue can promote decay of bone by bacteria. Microbiological decay of bone does not usually occur in environments that are waterlogged, arid, or permanently frozen, as these setting impede bacterial activity. Microbial decay results in specific decay patterns, known as microscopical focal destructions (MFDs). There are different types of MFDs, which, based on their morphology, are named linear longitudinal, budded or lamellate tunnelling. Some of these types may be visible in thin section (Figure 1.12b). It can be unclear whether the different morphologies of alteration indicate different species, different circumstances or different stages in bacterial attack (Jans 2014; see also Hedges & Millard 1995), although some MFD morphologies are characteristic of type or species of bone-degrading mechanisms (Trueman & Martill 2002; Jans 2005).

In noncalcareous environments with available moisture and oxygen, saprophytic fungi can colonize and degrade bone (see Forancelli *et al.* 2012). Fungal degradation can be recognized in thin section by visible fungal hyphae, or the occurrence of branching tunnels ('Wedl tunnels') that run through the bone tissue (Figure 1.12c) although some tunnelling ('Wedl type 2') may be of bacterial origin (Trueman & Martill 2002). In waterlogged settings, fungal decay is not possible; however, traces of fungal decay in these environments can indicate that the decay occurred prior to saturation, providing evidence for a change in soil environment. Bone submerged in shallow, clear water may become colonized by cyanobacteria. These microbes tend to tunnel into the outer bone layer (Figure 1.12d), sometimes leaving small spheres of hydroxylapatite behind in their cavities (Turner-Walker & Jans 2008; Turner-Walker 2012).

1.3.4 Chemical Weathering

The combination and special arrangement of collagen and carbonated hydroxylapatite in bones makes bone frequently more resistant to decay than other materials in the archaeological record (Collins *et al.* 2002).

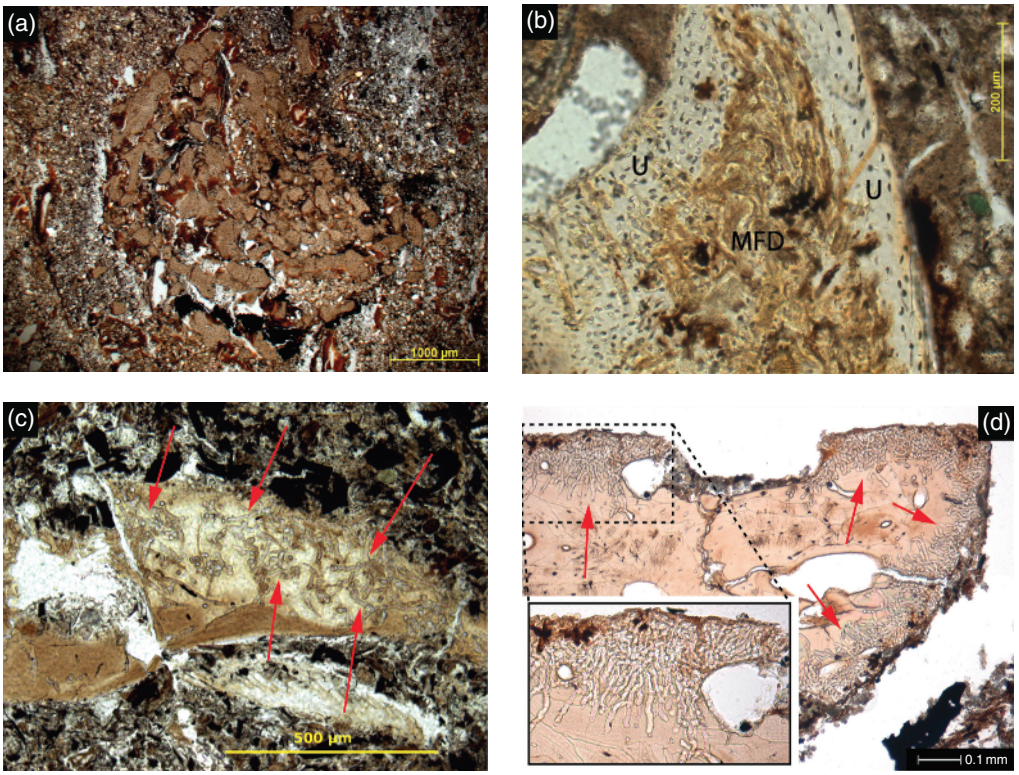

Figure 1.12 Bone degradation by biological agents. (a) Bone that has been fragmented, ingested and excreted by a worm. Note the crescent-shaped infill pattern that is typical for worm action. PPL. (b) Rodent skull with zone with bacterially induced microfocal destruction (MFD) in the centre, and unaltered bone (U) close to the bone surface. PPL. (c) Bone fragment with tunnels caused by fungal decay, some of the tunnels indicated by arrows (PPL). Middle Neolithic midden, Swifterbant S4 (The Netherlands – see Huisman *et al.* 2014a). (d) Tunnelling by cyanobacteria (some indicated by arrows) in the outer layer of a bone from a Swiss lakeshore dwelling. Note that the tunnelling is restricted to the 100–200 µm zone close to the surface. Inset shows detail of the tunnels. PPL. Image courtesy of K. Ismail-Meyer.

However, it is the combination of the bone structure, the preburial processing of bone (e.g., fresh bone versus cooked) and the characteristics of the burial environment (pH, temperature, water regime, and so forth) that determines the preservation, degradation or even complete disappearance of bones from archaeological sites (Hedges *et al.* 1995; Nicholson 1996; Nielsen-Marsh 2000; Jans 2004; Jans *et al.* 2002).

Chemical weathering of bone can result in additions to the bone tissue, reordering or recrystallization of constituents, loss of either the organic or inorganic portions, or complete dissolution of bone. As with other taphonomic processes, only some impacts are visible in bone fragments in thin section, but those that are can be informative about past burial environments.

1.3.4.1 Chemical Additions or Substitutions within Bone

Fossilization is a process of chemical alteration of bone following its abandonment on a surface or burial. Fossilization results in net increases and decreases in elemental abundance in bone relative to its fresh state (*in vivo*), with the exact ionic substitutions determined by the surrounding soil environment (Pate *et al.* 1989). Other diagenetic processes result in mineral additions or replacement within bone that can aid in its preservation, while oxide mineral staining can alter the colour of bone, mimicking the effects of other processes.

1.3.4.2 Staining

Bone may become stained with various components from the burial environment without complete replacement of the bone mineral. As noted by Shahack-Gross *et al.* (1997), it is important to distinguish colour changes from staining from those caused by heating. Bone may become (reddish) brown due to the precipitation of humic acids from soils that contain these components in abundance (e.g., peat). Microbial-enhanced processes can cause precipitation of iron(III) and manganese(IV) compounds (oxides, hydroxides, oxyhydroxides) in or on bone (Figure 1.13a, b). Staining by iron(III) produces a reddish to orange colour in PPL, which may be confused with colour change caused by heating (see above). The manganese(IV) minerals are commonly opaque in PPL,

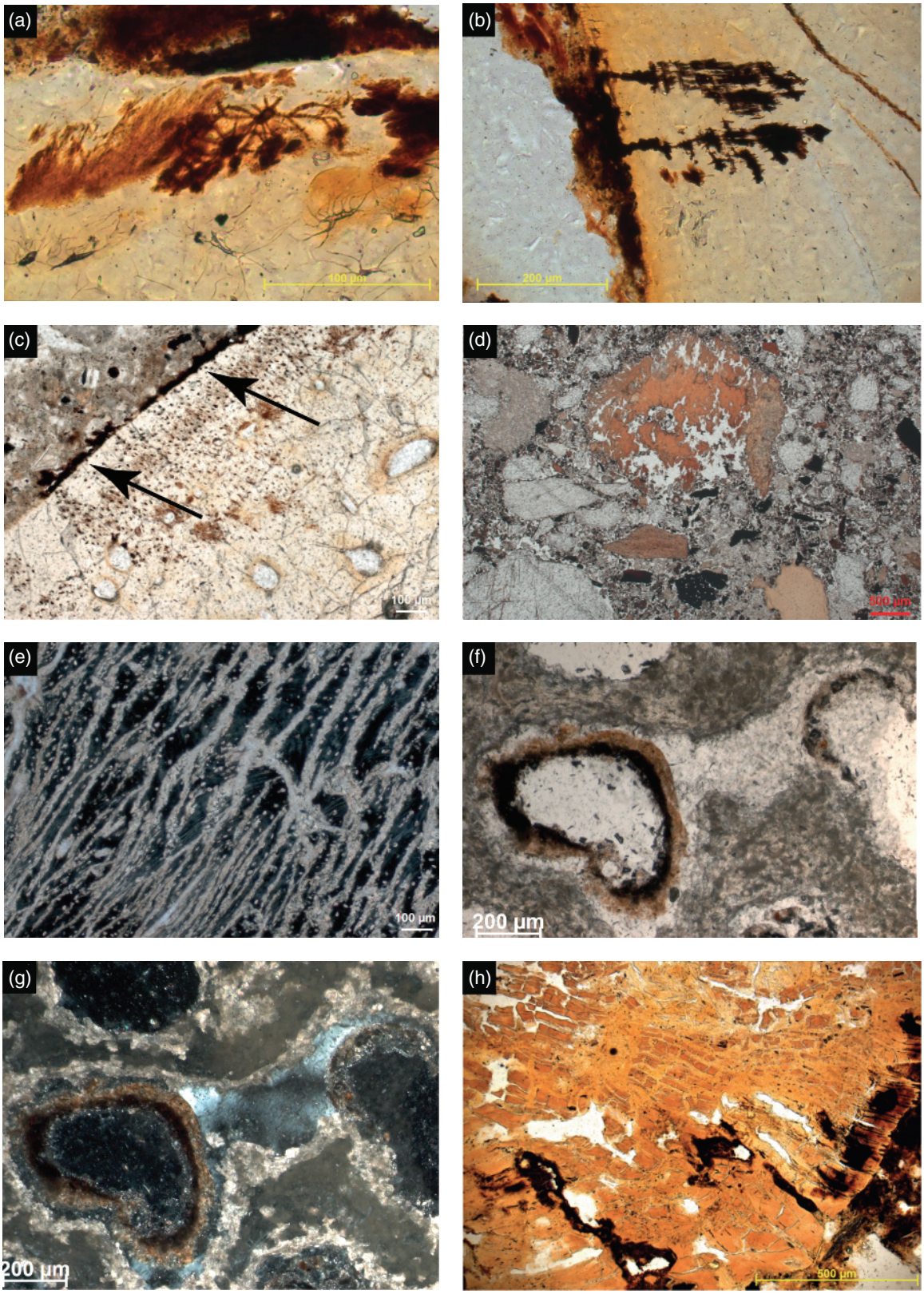

Figure 1.13 Bone stained by metal precipitates (a–c). (a) Iron oxides. PPL. (b) Manganese oxides. PPL. Note that both yellow to orange staining in the bone mass and the black coatings may be confused with heated bone. Medieval to nineteenth-century occupation layers, De Zuidert (The Netherlands). (c) Oxide staining (arrows) outside bone fragment caused by microbial activity. Aceramic Neolithic midden from Aşıklı Höyük (Turkey). Dissolution features and mineral neoformations (d–h). (d) Dissolution leading to total disintegration of the bone microstructure (PPL). Middle Stone Age deposits in Elands Bay Cave (South Africa). PPL. (e) Carbonate impregnating bone, Upper Palaeolithic deposits in Uçağızlı Cave I (Turkey). XPL. (f) and (g) Spongy bone replaced by calcite. Upper Palaeolithic deposits in Uçağızlı Cave I (Turkey): (f) PPL; (g) XPL. (h) Degradation resulting in shrinkage and fragmentation of the bone mass, forming elongated angular fragments. The resulting pore space is partially filled with newly formed phosphates. Medieval harbour sediments, Stavanger (Norway). PPL. Thin section courtesy of B. Sageidet.

and tend to form dendritic patterns as can be seen in Figure 1.13b. Bacterial activity in and around bones can result in oxide staining (Figure 1.13c; Shahack-Gross *et al.* 1997).

1.3.4.3 Recrystallization of Bone Mineral

Bioapatite is stable only when the pH of the burial environment is above 8.1. Bioapatite in fresh bone has low crystallinity (Paschalis *et al.* 1997). The stability of bioapatite is lower than that of geogenic hydroxlyalpatite, so in the pH range between 7 and 8.1 (and especially between 7 and 7.5) bone mineral will be replaced over time by hydroxylapatite with a higher crystallinity. This replacement can be monitored by several quantitative infrared and Raman indices, including the splitting factor (Weiner & Bar-Yosef 1990; Berna *et al.* 2004) and the crystallinity index (see Thompson *et al.* 2011), both of which can be modified for measurements made in thin section using FTIR microscopy (see Berna 2017, this book). Bone crystallinity can also be measured using x-ray diffraction (Pucéat *et al.* 2004), with measurements conducted in thin sections using micro-XRD (see Berthold & Mentzer 2017, this book). The effects of recrystallization are visible in thin section. According to Karkanas & Goldberg (2010), simple recrystallization of the bioapatite in bone results in complete or partial disappearance of the ropy structure, and its replacement by a mosaic-speckled b-fabric, with domains of ca. 50 µm in diameter.

1.3.4.4 Dissolution of Bone

Both the organic and inorganic components of bone can be impacted by postdepositional decomposition, dissolution and leaching. As reviewed by Collins *et al.* (2002), these processes are often mediated by microbial activity and can occur independently, in sequence, or at the same time. The mechanisms and rates of deterioration are determined by burial environment. In some cases, losses are balanced by gains, as in collagen loss causing increased porosity, which in turn is infilled by mineral. In other cases, dissolution of one component allows the acceleration or loss of the other.

Removal of Collagen and Other Organic Material Collins *et al.* (2002) outline several pathways for the decomposition and removal of organic material from bone. First, loss of collagen by hydrolysis occurs under extremes of pH with rates increased by high temperatures. Hydrolysis yields gelatin, which can be flushed from the bone under most burial conditions. Second, collagen may be subject to microbial attack, a process that is accelerated at neutral pH. Collagen loss from bone may be observed in thin section as a decrease in birefringence strength and change in elongation sign (see above).

Acid-Induced Dissolution of Bone Mineral In burial environments with sediment moisture of pH <7, bones can dissolve completely. In oxygenated acidic to neutral conditions (including acid sulphate soils and guano-rich cave deposits), coupled decay of the bone collagen and dissolution of the bone mineral matrix may cause complete bone loss (Berna *et al.* 2004). Dissolution processes as observed in thin section may start as a simple loss of birefringence, progressing to flaking and loss of recognizable features and, in its most extreme form, total disintegration of the microstructure (generalized destruction; Garland 1993) and loss of the bone mass (see Figure 1.13d). The low pH conditions that promote bone dissolution can be widespread throughout the deposit, or localized due to the presence of organic acids.

In special cases, apatite in bone buried in waterlogged acidic soils may dissolve while the collagen remains present, although the collagen may be transformed into gelatine. This is specifically the case in environments like peat bogs or other acidic environments (Milner *et al.* 2011; Turner-Walker & Peacock 2008).

1.3.4.5 Coupled Dissolution and Mineral Neoformation

In some archaeological contexts, bone mineral dissolution may occur in association with secondary mineral formation. The minerals may replace the bone, forming crystal aggregates that are pseudomorphic after the original bone tissue (e.g., the replacement of bone mineral by calcite: see Figure 1.13e–g; and the replacement of bone mineral by kutnohorite: see Berthold & Mentzer 2017, this book). Alternatively, bone dissolution can release phosphate into the sediment, which later becomes incorporated into secondary minerals (Figure 1.13h). Dissolution and mineral neoformation pathways are varied and complex and dependent on depositional setting.

Cave and Rock Shelter Settings In cave deposits – especially if the caves are inhabited by insectivorous bats – high concentrations of phosphate from guano, dung or decaying organic material, in combination with acidic conditions, may result in the dissolution of bone mineral while new phosphate minerals are formed (e.g., carbonate-rich hydroxylapatite, taranakite and montgomeryite; Goldberg & Nathan 1975; Schiegl *et al.* 1996; Karkanas *et al.* 2000; Stiner *et al.* 2001; Weiner *et al.* 2002; Shahack-Gross *et al.* 2004). This type of dissolution may be the reason for the lateral and vertical variability in preservation and disappearance of bone from some cave sediments (Karkanas *et al.* 2000; Shahack-Gross *et al.* 2004). Phosphate-induced dissolution forms cavities in the bone mass, while newly formed phosphate minerals can precipitate in crusts surrounding the bone proper (see Figure 1.13d). In some

thin sections, this relationship between authigenic phosphate minerals and bone can be documented. In other cases, authigenic phosphate minerals are present in samples where bone is entirely absent. These minerals may be identified in thin section using optical properties and crystal habit, with mineralogical identifications confirmed directly using FTIR microscopy, micro-XRD, or indirectly using elemental analyses (e.g., micro-XRF). It is tempting to regard all secondary phosphates as being derived directly from the decay of bone; however, the reality is more nuanced. Although many minerals have been documented in cave contexts where bones are absent or poorly preserved (e.g., montgomeryite, leucophosphite, variscite, newberyite and taranakite; Karkanas *et al.* 2000, 2002; Weiner *et al.* 2002) all have been identified in nonanthropogenic guano deposits (Hill & Forti 1997). Mineral stability diagrams may be informative for reconstructing general sedimentary conditions (e.g., Karkanas *et al.* 2000; Karkanas 2010) but in many cases it will be impossible to distinguish secondary minerals formed with guano-derived phosphates from those formed with bone-derived phosphate.

Open-Air Contexts Outside of cave settings, vivianite has been documented in association with archaeological bone. This iron phosphate ($Fe(II)_3PO_4$) is easily identifiable due to its bright blue colour in PPL and pleochroism when oxidized. Vivianite frequently occurs as a neoformed phosphate in bones from waterlogged environments (Gebhardt & Langohr 1999; Simpson *et al.* 2005; McGowan & Prangnell 2006; Macphail 2008; Macphail & Cruise 2009). Like the minerals described above, it is not clear if the source of phosphate in vivianite is derived from bone. The conditions under which vivianite forms (reducing conditions, high nutrient levels and pH 6-8.5; Nriagu & Dell 1974; Postma 1977) are in general not conducive to dissolution of bone mineral.

In other open contexts, phosphatic pedofeatures such as void infillings have been documented. In fish and shell middens from the coast of Brazil, neoformed calcium phosphates are common in the micromass and as pedofeatures (coatings and infillings). These features likely derive both from the biochemical weathering of the fish bone mineral and from decay of soft animal tissue (Villagran *et al.* 2009, 2010; Corrêa *et al.* 2013; Villagran 2014). Adderley *et al.* (2004) conducted crystallinity measurements on similar Ca-Fe phosphate infillings in an archaeological site using microfocus synchrotron X-ray scattering analyses. He demonstrated that the neoformed phosphates had very similar properties to fish bones.

Finally, certain types of soils, such as the *terra preta* soils from Amazonia (see Arroyo-Kalin 2017, this book), are hypothesized to have been initially rich in organic materials and bone. Calcium-phosphate minerals, also combined with iron and aluminium, have been described in micromorphological samples of *terra preta* (Lima *et al.* 2002; Schaefer *et al.* 2004). Schaefer *et al.* (2004) proposed that these minerals derive from the faunal digestion of calcium-phosphates from bones. Similar infillings and coatings composed of calcium-iron-phosphates are common pedofeatures found in moist, temperate and sub-boreal climates in acidic soils. These have been described in diverse contexts as pedofeatures with both crystallitic or undifferentiated b-fabrics, and researchers speculate that they derived from bone alteration (Jenkins 1994; Simpson *et al.* 2000; Adderley *et al.* 2004; Macphail 2008).

1.4 Guidelines for Micromorphological Analysis

Below we provide a general guideline of key points that one should note when describing bones in thin section, with the goal of using these observations for reconstructing site formation processes.

- Bones should be treated as part of the coarse fraction and describe them as such, following the guidelines developed by Stoops (2003). Note the following:
  - whether the bone fragments consist of cortical or spongy bone;
  - their size and size distribution (sorting);
  - their frequency and distribution throughout the thin section (e.g., in discrete microstratigraphic units, or evenly dispersed throughout);
  - morphology of bones, particularly the degree of roundness;
  - if elongate in form, describe any preferred orientation or apparent fabric.
- These characteristics of the bones can be useful for assessing mode of deposition or possible postdepositional disturbance (e.g., bioturbation).
- Note if there is any mechanical breakage of the bone. Determine if the mechanical breakage is a result of:
  - secondary mineral formation within the bone;
  - trampling caused by human or animal occupation of the site.

By noting any processes of mechanical breakage, the micromorphologist can assess possible chemical diagenetic processes influencing the preservation of bone at the site. If human- or animal-induced breakage can be identified, the researcher can identify former buried surfaces or floors, or even assess variation in use of space within a site.

- Note if any of the bone fragments appears burnt. It may be necessary to use other microanalytical techniques, such as FTIR microscopy, to establish if the bones are burnt, and to what degree. In particular, note the following:
  - relative degree of burning, whether unburnt, charred or calcined;
  - proportion of bone fragments that appear burnt relative to those that appear charred or calcined;
  - the spatial relationship of burnt bones to other sedimentary components and pedofeatures, particularly the relationship to other bones that do not appear burnt.

By describing these characteristics, the micromorphologist can assess the role that fire played in the formation of the site. By noting the spatial relationship between burnt and unburnt bone, he or she can also determine if the burnt bone fragments constitute evidence for in situ combustion, or if they were transported or redeposited following burning.

- Note any alteration to the bone, including:
  - Has it been stained, and if so, is it stained by iron oxides, manganese oxides, or both?
  - Is there any pitting that may indicate biological alteration of the bone?
  - Is there any evidence of recrystallization or dissolution of the bone? Identification of minerals replacing bone may need to be augmented with other microanalytical techniques (FTIR microscopy, micro-XRD, micro-probe or SEM).
  - Are any secondary minerals present that may have formed through alteration, dissolution and reprecipitation of bone apatite? Identification of these minerals may require the application of additional microanalytical techniques.

The study of bone alteration and diagenesis can help assess past chemical conditions within archaeological sites, with implications for understanding the preservation of various classes of artefacts within the archaeological record.

References

Adderley, W. P., Alberts, I. L., Simpson, I. *et al.* (2004) Calcium–iron–phosphate features in archaeological sediments: Characterization through microfocus synchrotron X-ray scattering analyses. Journal of Archaeological Science 31, 1215–1224.

Altemüller, H. J. & Van Vliet-Lanoe, B. (1990) Soil thin section fluorescence microscopy. In: Douglas, L. A. (ed.) Soil Micromorphology: A basic and Applied Science. Elsevier, Amsterdam, pp. 565–579.

Arroyo-Kalin, M. (2017) Amazonian Dark Earth. In: Nicosia, C. & Stoops, G. (eds) Archaeological Soil and Sediment Micromorphology. John Wiley & Sons, Ltd, Chichester, pp. 345–357.

Backwell, L. R., Parkinson, A. H., Roberts, E. M. *et al.* (2012) Criteria for identifying bone modification by termites in the fossil record. Palaeogeography, Paleoclimatology, Palaeoecology 337–338, 72–87.

Behrensmeyer, A. K. (1978) Taphonomic and ecologic information from bone weathering. Paleobiology 4 (2), 150–162.

Bennett, J. L. (1999) Thermal alteration of buried bone. Journal of Archaeological Science 26, 1–8.

Berna, F. (2017) FTIR microscopy. In: Nicosia, C. & Stoops, G. (eds) Archaeological Soil and Sediment Micromorphology. John Wiley & Sons, Ltd, Chichester, pp. 411–415.

Berna, F. & Goldberg, P. (2008) Assessing Paleolithic pyrotechnology and associated hominin behavior in Israel. Israel Journal of Earth Sciences 56, 107–121.

Berna, F., Goldberg, P., Horwitz L. K. *et al.* (2012) Microstratigraphic evidence of in situ fire in the Acheulean strata of Wonderwerk Cave, Northern Cape province, South Africa. Proceedings of the National Academy of Sciences of the United States of America 109, E1215-20.

Berna, F., Matthews, A. & Weiner, S. (2004) Solubilities of bone mineral from archaeological sites: The recrystallization window. Journal of Archaeological Science 31, 867–882.

Berthold & Mentzer (2017) X-ray Microdiffraction. In: Nicosia, C. & Stoops, G. (eds) Archaeological Soil and Sediment Micromorphology. John Wiley & Sons, Ltd, Chichester, pp. 417–429.

Bertram, J. E. & Gosline, J. M (1986) Fracture toughness design in horse hoof keratin. Journal of Experimental Biology 125, 29–47.

Bourne, G. H. (1956) The Biochemistry and Physiology of Bone. Academic Press, New York.

Bromage, T. G., Goldman, H. M., McFarlin, S. C. *et al.* (2003) Circularly polarized light standards for investigations of collagen fiber orientation in bone. The Anatomical Record (Part B: New Anathomy) 274B, 157–168.

Brönnimann, D., Pümpin, C., Ismail-Meyer, K. *et al.* (2017) Excrements of omnivores and carnivores. In: Nicosia, C. & Stoops, G. (eds) Archaeological Soil and Sediment Micromorphology. John Wiley & Sons, Ltd, Chichester, pp. 67–81.

Brunner, H. & Coman, B. (1974) The Identification of Mammalian Hairs. Inkata Press, Melbourne.

Carlson, S. J. (1990) Vertebrate dental structures. In: Carter, J. G. (ed.), Skeletal Biomineralization: Patterns, Processes and Evolutionary Trends. Van Nostrand Reinhold, New York, pp. 531–556.

Clark, J. L. & Ligouis, B. (2010) Burned bone in the Howieson's Poort and post-Howieson's Poort Middle Stone Age deposits at Sibudu (South Africa): Behavioral and taphonomic implications. Journal of Archaeological Science 37, 2650–2661.

Collins, M. J., Nielsen-Marsh, C. M., Hiller, J. *et al.* (2002) The survival of organic matter in bone: A review. Archaeometry 44, 383–394.

Conard, N. J. (1992) Tönchesberg and its position in the Paleolithic prehistory of Northern Europe. Monograph 20, Römisch-Germanisches Zentralmuseum Series. Habelt, Bonn.

Corrêa, G. R., Schaefer, C. E. & Gilkes, R. J. (2013) Phosphate location and reaction in an archaeoanthrosol on shell-mound in the Lakes Region, Rio de Janeiro State, Brazil. Quaternary International 315, 16–23.

Courty, M. A., Goldberg, P. & Macphail, R. I. (1989) Soils and Micromorphology in Archaeology. Cambridge University Press, Cambridge.

Currey, J. D. (2002) Bones. Structure and Mechanics. Princeton University Press, Princeton.

Dejmal, M., Lisá, L., Nývltová, M. F. *et al.* (2014) Medieval horse stable: The results of multi proxy interdisciplinary research. PloS one 9(3) e89273. doi: 10.1371/journal.pone.0089273

Dibble, H. L., Berna, F., Goldberg, P. *et al.* (2009) A preliminary report on Pech de l'Azé IV, layer 8 (Middle Paleolithic, France). PaleoAnthropology 8, 182–219.

Ellingham, S. T. D., Thompson, T. J. U., Islam, M. *et al.* (2015) Estimating temperature exposure of burnt bone – a methodological review. Science and Justice 55, 181–188.

Estévez, J., Villagran, X. S., Balbo, A. *et al.* (2014) Microtaphonomy in archaeological sites: The use of soil micromorphology to better understand bone taphonomy in archaeological contexts. Quaternary International 330, 3–9.

Forancelli, L. M. A., Villagran, X. S. V. & Martins, G. R. (2012) Macroscopic and microbiological alterations of bird and mammal bones buried in a Cerrado biome (south western Brazil). Journal of Archaeological Science 39, 1394–1400.

Francillon-Vieillot, H., De Buffrénil, V., Castanet, J. *et al.* (1990) Microstructure and mineralization of vertebrate skeletal tissue. In: Carter, J. G. (ed.) Skeletal biomineralization: patterns, processes and evolutionary trends. Van Nostrand Reinhold, New York, pp. 471–530.

Garland, A. N. (1993) An introduction to the histology of exhumed mineralised tissue. In: Grupe, G. & Garland, A. N. (eds) Histology of Ancient Bone: Methods and Diagnosis. Springer Verlag, Berlin.

Gebhardt, A., Langohr, R. (1999) Micromorphological study of construction materials and living floors in the medieval motte of Werken (West Flanders, Belgium). Geoarchaeology 14, 595–620.

Goldberg, P. & Berna, F. (2010) Micromorphology and context. Quaternary International 214, 56–62.

Goldberg, P., Dibble, H., Berna, F. *et al.* (2012) New evidence on Neandertal use of fire: Examples from Roc de Marsal and Pech de l'Azé IV. Quaternary International 247, 325–340.

Goldberg, P., Miller, C. E., Schiegl, S. *et al.* (2009) Bedding, hearths, and site maintenance in the Middle Stone Age of Sibudu Cave, KwaZulu-Natal, South Africa. Archaeological and Anthropological Sciences 1, 95–122.

Goldberg, P. & Nathan, Y. (1975) The phosphate mineralogy of et Tabun cave, Mount Carmel, Israel. Mineralogical Magazine 40, 253–258.

Goss, R. J. (1983) Deer Antlers: Regeneration, Function, and Evolution. Academic Press, New York.

Hanson, M. & Cain, C. R. (2007) Examining histology to identify burned bone. Journal of Archaeological Science 34, 1902–1913.

Hashiguchi, K. & Hashimoto, K. (1995) The mineralization of crystalline inorganic components in Japanese serow horn. Okajimas Folia Anatomica Japonica 72, 235–244.

Hashiguchi, K., Hashimoto, K. & Akao, M. (2001) Morphological character of crystalline components present in saiga horn. Okajimas Folia Anatomica Japonica 78, 43–48.

Heckel, C. (2009) Physical characteristics of mammoth ivory and their implications for ivory work in the Upper Paleolithic. Mitteilungen der Gesellschaft für Urgeschichte 18, 71–91.

Hedges, R. E. M. (2002) Bone diagenesis: An overview of processes. Archaeometry 44, 319–328.

Hedges, R. E. M. & Millard, A. R. (1995) Bones and groundwater: towards the modelling of diagenetic processes. Journal of Archaeological Science 22, 155–164.

Hedges, R., Millard, A. R. & Pike, A. W. G. (1995) Measurements and relationships of diagenetic alteration of bone from three archaeological sites. Journal of Archaeological Science 22, 201–209.

Hill, C. & Forti, P. (1997) Cave Minerals of the World. 2nd ed. National Speleological Society, Huntsville.

Hillier, M. L. & Bell, M. S. (2007) Differentiating human bone from animal bone: A review of histological methods. Journal of Forensic Science 52, 249–263.

Hoke, N., Burger, J., Weber, C. *et al.* (2011) Estimating the chance of success of archaeometric analyses of bone: UV-induced bone fluorescence compared to histological screening. Palaeogeography, Palaeoclimatology, Palaeoecology 310, 23–31.

Hollund, H. I. (2013) Diagenetic Screening of Bone Samples; Tools to Aid Taphonomic and Archaeometric Investigations. Geoarchaeological and Bioarchaeological Studies 15. Vrije Universiteit, Amsterdam.

Huchet, J.-B., Deverley, D., Gutierrez, B. *et al.* (2011) Taphonomic evidence of a human skeleton gnawed by termites in a Moche-civilisation graven at Huaca de la Luna, Peru. International Journal of Osteoarchaeology 21, 92–102.

Huisman, D. J., Brounen, F., Lohof, E. *et al.* (2014a) Micromorphological study of Early Neolithic (LBK) soil features in the Netherlands. Journal of Archaeology in the Low Countries 5, 107–133.

Huisman, D. J., Jongmans, A. G, Raemaekers, D. C. M. (2009) Investigating Neolithic land use in Swifterbant (NL) using micromorphological techniques. Catena 78, 185–197.

Huisman, D. J., Ngan-Tillard, D. J. M., Tensen, M. A. *et al.* (2014b) A question of scales: studying Neolithic subsistence using micro CT scanning of midden deposits. Journal of Archaeological Science 49, 585–594.

Jans, M. (2004) Characterisation of microbial attack on archaeological bone. Journal of Archaeological Science 31, 87–95.

Jans, M. (2005) Histological Characterisation of Diagenetic Alteration of Archaeological Bone. Geoarchaeological and Bioarchaeological Studies 4. Vrije Universiteit, Amsterdam.

Jans, M. (2014) Microscopic destruction of bone. In: Pokines, J. Symes, S. A. & Roper, C. (eds) Manual of Forensic Taphonomy. CRC Press, Boca Raton, pp. 19–35.

Jans, M., Kars, H., Nielsen-Marsh, C. M. *et al.* (2002) In situ preservation of archaeological bone: A histological study within a multidisciplinary approach. Archaeometry 3, 343–352.

Jenkins, D. (1994) Interpretation of interglacial cave sediments from a hominid site in North Wales: Translocation of Ca-Fe-phosphates. In: Ringrose-Coase, A. & Humphreys, G. (eds) Soil Micromorpholoy: Studies in Management and Genesis. Elsevier, Amsterdam, pp. 293–305.

Karkanas, P. (2010) Preservation of anthropogenic materials under different geochemical processes: A mineralogical approach. Quaternary International 214, 63–69.

Karkanas P., Bar-Yosef O., Goldberg P. *et al.* (2000) Diagenesis in prehistoric caves: The use of minerals that form in situ to assess the completeness of the archaeological record. Journal of Archaeological Science 10, 915–929.

Karkanas. P. & Goldberg, P. (2010) Phosphatic features. In: Stoops, G., Marcelino, V., & Mees, F. (eds) Interpretation of Micromorphological Features of Soils and Regoliths, Elsevier, Amsterdam, pp. 521–537.

Karkanas, P., Rigaud, J-P., Simek, J. F. *et al.* (2002) Ash bones and guano: A study of the minerals and phytoliths in the sediments of Grotte XVI, Dordogne, France. Journal of Archaeological Science 29, 721–732.

Karkanas, P., Shahack-Gross, R., Ayalon, A. *et al.* (2007) Evidence for habitual use of fire at the end of the Lower Paleolithic: Site-formation processes at Qesem Cave, Israel. Journal of Human Evolution 53, 197–212.

Kasapi, M. A. & Gosline, J. M (1997) Design complexity and fracture control in the equine hoof wall. Journal of Experimental Biology 200, 1639–1659.

Lebon, M., Reiche, I. & Bahain, J.-J. (2010) New parameters for the characterization of diagenetic alterations and heat-induced changes of fossil bone mineral using Fourier transform infrared spectrometry. Journal of Archaeological Science 37, 2265–2276.

Lima, H., Schaefer, C. E. G. R., Mello, J. W. V. *et al.* (2002) Pedogenesis and pre-Colombian land use of 'Terra Preta Anthrosols' ('Indian black earth') of Western Amazonia. Geoderma 110, 1–17.

Lindsay, W. L., Vlek, P. L. G. & Chien, S. H. (1989) Phosphate Minerals. In: Dixon, J. B. & Weed, S. B. (eds) Minerals in Soil Environments. 2nd edition. Soil Science Society of America, Madison, pp. 1089–1130.

Linse, A. R. (1992) Is bone safe in a shell midden? In: Stein, J. K. (ed.) Deciphering a Shell Midden. Academic Press, San Diego, pp. 327–345.

Lowenstam, H. A. & Weiner, S. (1989) On Biomineralization. Oxford University Press, New York.

Macphail, R. I. (2008) Soils and archaeology. In: Pearsall, D. M. (ed.) Encyclopedia of Archaeology. Academic Press, New York, pp. 2064–2072.

Macphail, R. I. & Cruise, J. (2001) The soil micromorphologist as team player. A multianalytical approach to the study of European microstratigraphy. In: Goldberg, P., Holliday, V. T. & Ferring, C. R. (eds) Earth Sciences and Archaeology. Kluwer Academic / Plenum Publishers, New York, pp. 241–267.

Macphail, R. I. & Goldberg, P. (2010) Archaeological materials. In: Stoops, G., Marcelino, V. & Mees, F. (eds) Interpretation of Micromorphological Features of Soils and Regoliths. Elsevier, Amsterdam, pp. 589–622.

Mallol, C., Mentzer, S. M. & Miller, C. E. (2017) Combustion features. In: Nicosia, C. & Stoops, G. (eds) Archaeological Soil and Sediment Micromorphology. John Wiley & Sons, Ltd, Chichester, pp. 299–330.

Mallol, C., Mentzer, S. M. & Wrinn, P. J. (2009) A micromorphological and mineralogical study of site formation processes at the late Pleistocene site of Obi-Rakhmat, Uzbekistan. Geoarchaeology 24, 548–575.

McCutcheon, P. T. (1992) Burned archaeological bone. In: Stein, J. K. (ed.) Deciphering a Shell Midden. Plenum Press, San Diego, pp. 347–370.

McGowan, G. & Prangnell, J. (2006) The significance of vivianite in archaeological settings. Geoarchaeology 21, 93–111.

Mentzer, S. M., Voyatzis, M. & Romano, D. G. (2015) Micromorphological contributions to the study of ritual behavior at the Ash Altar to Zeus on Mt. Lykaion, Greece. Archaeological and Anthropological Sciences. DOI: 10.1007/s12520-014-0219-y

Miller, C. E. (2015) A Tale of Two Swabian Caves. Kerns-Verlag, Tübingen.

Miller, C. E., Conard N. J., Goldberg P. *et al.* (2009) Dumping, sweeping and trampling: experimental micromorphological analysis of anthropogenically modified combustion features. In: Théry-Parisot, I. Chabal, L. & Costamagno, S. (eds) The Taphonomy of Burned Organic Residues and Combustion Features in Archaeological Contexts. Proceedings of the Round Table, Valbonne, May 27-29 2008. P@lethnologie 2, 25–37.

Miller, C. E., Goldberg, P. & Berna, F. (2013) Geoarchaeological investigations at Diepkloof Rock Shelter, Western Cape, South Africa. Journal of Archaeological Science 40, 3432–3452.

Milner, N., Conneller, C., Elliott, B. *et al.* (2011) From riches to rags: Organic deterioration at Star Carr. Journal of Archaeological Science 38, 2818–2832.

Ngan-Tillard, D. & Huisman, H. (2017) Micro-CT scanning. In: Nicosia, C. & Stoops, G. (eds) Archaeological Soil and Sediment Micromorphology. John Wiley & Sons, Ltd, Chichester, pp. 441–449.

Nicholson, R. A. (1993) A morphological investigation of burnt animal bone and an evaluation of its utility in archaeology. Journal of Archaeological Science 20, 411–428.

Nicholson, R. A. (1996) Bone degradation, burial medium and species representation: Debunking the myths, an experiment-based aproach. Journal of Archaeological Science 23, 513–533.

Nielsen-Marsh, C. (2000) Patterns of diagenesis in bone II: Effects of acetic acid treatment and the removal of diagenetic $CO^{2}_{3}{}^{-}$. Journal of Archaeological Science 27, 1151–1159.

Nriagu, J. O. & Dell, C. I. (1974) Diagenetic formation of iron phosphates in recent lake sediments, American Mineralogist 59, 934–946.

O'Conor, S., Solazzo, C. & Collins, M. (2015) Advances in identifying archaeological traces of horn and other keratinous tissues. Studies in Conservations 60, 393–417.

Paschalis, E. P., Betts, F., DiCarlo, E. *et al.* (1997) FTIR microspectroscopic analysis of normal human cortical and trabecular bone. Calcified Tissue International 61, 480–486.

Pate, F. D., Hutton, J. T. (1988) The use of soil chemistry data to address post-mortem diagenesis in bone mineral. Journal of Archaeological Science 15, 729–739.

Pate, F. D., Hutton, J. T., & Norrish, K. (1989) Ionic exchange between soil solution and bone: Toward a predictive model. Applied Geochemistry 4, 303–316.

Piga, G., Malgosa, A., Thompson, T. J. U. *et al.* (2008) A new calibration of the XRD technique for the study of archaeological burned human remains. Journal of Archaeological Science 35, 2171–2178.

Posner, A. S., Blumenthal, N. C. & Betts, F. (1984) Chemistry and structure of precipitated hydroxyapatites. In: Nriagu, J. O. & Moore, P. B. (eds) Phosphate Minerals. Springer-Verlag, Berlin, pp. 330–349.

Postma, D. (1977) The occurrence and chemical composition of recent Fe-rich carbonates in a river bog. Journal of Sedimentary Petrology 47, 1089–1098.

Provenza, D. V. & Seiber, W. (1986) Oral Histology: Inheritance and Development. Lea & Febiger, Philadelphia.

Pucéat, E., Reynard, B. & Lécuyer, C. (2004) Can crystallinity be used to determine the degree of chemical alteration of biogenic apatites? Chemical Geology 205, 83–97.

Reiche, I. (2010) Heating and diagenesis-induced heterogeneities in the chemical composition and structure of archaeological bones from the Neolithic site of Chalain 19 (Jura, France). P@lethonologie 10, 129–144.

Roberts, S. J., Smith, C. I., Millard, A. *et al.* (2002) The taphonomy of cooked bone: Characterizing boiling and its physico-chemical effects. Archaeometry 44, 485–494.

Salamon, J. C. (ed.) (1999) Concise Polymeric Materials Encyclopedia. CRC Press, Boca Raton.

Schaefer, C. E. G. R., Lima, H. N., Gilkes, R. J. *et al.* (2004) Micromorphology and electron microprobe analysis of phosphorus and potassium forms of an Indian Black Earth (IBE) Anthrosol from Western Amazonia. Australian Journal of Soil Research 42, 401–409.

Schiegl, S., Goldberg, P., Bar-Yosef, O. *et al.* (1996) Ash deposits in Hayonim and Kebara Caves, Israel: Macroscopic, microscopic and mineralogical observations, and their archaeological implications, Journal of Archaeological Science 23, 763–781.

Schiegl, S., Goldberg, P., Pfretzschner, H.-U. *et al.* (2003) Palaeolithic burnt bone horizons from the Swabian Jura: Distinguishing between in situ fireplaces and dumping areas. Geoarchaeology 5, 541–565.

Schmidt, W. J. & Keil, A. (1971) Polarizing Microscopy of Dental Tissues: Theory, Methods and Results from the Structural Analysis of Normal and Diseased Hard, Dental Tissues and Tissues Associated with them in Man and Other Vertebrates. Pergamon Press, Oxford.

Schoeninger, M., Moore, K., Murray, M. *et al.* (1989) Detection of bone preservation in archaeological and fossil samples. Applied Geochemistry 4, 281–292.

Shahack-Gross, R., Bar-Yosef, O. & Weiner, S. (1997) Black-coloured bones in Hayonim Cave, Israel: Differentiating between burning and oxide staining. Journal of Archaeological Science 24, 439–446.

Shahack-Gross, R., Berna, F., Karkanas, P. *et al.* (2004) Bat guano and preservation of archaeological remains in cave sites. Journal of Archaeological Science 31, 1259–1272.

Shipman, P., Foster, G. & Schoeninger, M. (1984) Burnt bones and teeth: An experimental study of colour, morphology, crystal structure and shrinkage. Journal of Archaeological Science 2, 307–325.

Simpson, I., Barrett, J. H. & Milek, K. B. (2005) Interpreting the Viking Age to Medieval period transition in Norse Orkney through cultural soil and sediment analyses. Geoarchaeology 20, 355–377.

Simpson, I., Perdikaris, S., Cook, G. *et al.* (2000) Cultural sediment analyses and transitions in early fishing activity at Langenesvaeret, Vesteralen, Northern Norway. Geoarchaeology 15, 743–763.

Smith, C., Nielsenmarsh, C., Jans, M. *et al.* (2007) Bone diagenesis in the European Holocene I: Patterns and mechanisms. Journal of Archaeological Science 34, 1485–1493.

Squires, K. E., Thompson, T. J. U., Islam, M. *et al.* (2011) The application of histomorphometry and Fourier Transform Infrared Spectroscopy to the analysis of early Anglo-Saxon burned bone. Journal of Archaeological Science 38, 2399–2409.

Stiner, M. C., Kuhn, S. L., Surovell, T. A. *et al.* (2001) Bone preservation in Hayonim Cave (Israel): A macroscopic and mineralogical study. Journal of Archaeological Science 28, 643–659.

Stiner, M. C., Kuhn, S. L., Weiner, S. *et al.* (1995) Differential burning, recrystallization and fragmentation of archaeological bone. Journal of Archaeological Science 22, 223–237.

Stoops, G. (2003) Guidelines for Analysis and Description of Soil and Regolith Thin Sections. Soil Science Society of America, Madison.

Su, X. W. & Cui, F. Z. (1999) Hierarchical structure of ivory: From nanometre to centimetre. Materials Science Engineering C7, 19–29.

Symes, S. A., Rainwater, C. W., Chapman, E. N. *et al.* (2008) Patterned thermal destruction of human remains in a forensic setting. In: Schmidt, C. W. & Symes, S. A. (eds) The Analysis of Burned Human Remains. Academic Press, London, pp. 15–54.

Szpak, P. (2011) Fish bone chemistry and ultrastructure: implications for taphonomy and stable isotope analysis. Journal of Archaeological Science 38, 3358–3372.

Théry-Parisot, I. (2002) Fuel management (bone and wood) during the Lower Aurignacian in the Pataud Rock Shelter (Lower Palaeolithic, Les Eyzies de Tayac, Dordogne, France). Contribution of Experimentation. Journal of Archaeological Science 29, 1415–1421.

Thompson, T. J. U., Gauthier, M. & Islam, M. (2009) The application of a new method of Fourier Transform Infrared Spectroscopy to the analysis of burned bone. Journal of Archaeological Science 36, 910–914.

Thompson, T. J. U., Islam, M., Piduru, K. *et al.* (2011) An investigation into the internal and external variables acting on crystallinity index using Fourier Transform Infrared Spectroscopy on unaltered and burned bone. Palaeogeography, Palaeoclimatology, Palaeoecology 299, 168–174.

Tombolato, L., Novitskaya, E. E., Chen, P. Y. *et al.* (2010) Microstructure, elastic properties and deformation mechanisms of horn keratin. Acta Biomaterialia 6, 319–330.

Tridico, S. R., Houck, M. M., Kirkbride, K. P. *et al.* (2014) Morphological identification of animal hairs: Myths and misconceptions, possibilities and pitfalls. Forensic Science International 238, 101–107.

Trueman, C, Behrensmeyer, A. K., Tuross, N. *et al.* (2004) Mineralogical and compositional changes in bones exposed on soil surfaces in Amboseli National Park, Kenya: Diagenetic mechanisms and the role of sediment pore fluids. Journal of Archaeological Science 31, 721–739.

Trueman, C. & Martill, D. M. (2002) The long-term survival of bone: The role of bioerosion. Archaeometry 44, 371–382.

Turner-Walker, G. (2012) Early bioerosion in skeletal tissue: Persistence through deep time. Neues Jahrbuch für Geologie und Paläontologie, Abhandlungen 256, 165–183.

Turner-Walker, G. & Jans, M. M. E. (2008) Reconstructing taphonomic histories using histological analysis. Palaeogeography, Palaeoclimatology, Palaeoecology 266, 227–235.

Turner-Walker, G. & Peacock, E. E. (2008) Preliminary results of bone diagenesis in Scandinavian bogs. Palaeogeography, Palaeoclimatology, Palaeoecology 266, 151–159.

Villagran, X. S. (2014) A redefinition of waste: Deconstructing shell and fish mound formation among

coastal groups of southern Brazil. Journal of Anthropological Archaeology 36, 211–227.
Villagran, X. S., Giannini, P. C. F. & DeBlasis, P. (2009) Archaeofacies analysis: Using depositional attributes to identify anthropic processes of deposition in a monumental shell mound of Santa Catarina State, southern Brazil. Geoarchaeology 24, 311–335.
Villagran, X. S., Klokler, D., Nishida, P. *et al.* (2010) Lecturas estratigraficas: arquitetura funeraria y depositación de residuos en el sambaquí Jabuticabeira II. Latin American Antiquity 21, 195–216.
Villagran, X. S., Schaefer, C. E. G. R. & Ligouis, B. (2013) Living in the cold: Geoarchaeology of sealing sites from Byers Peninsula (Livingston Island, Antarctica). Quaternary International 315, 184–199.
Virág, A. (2012) Histogenesis of the unique moprhology of Proboscidean Ivory. Journal of Morphology 273, 1406–1423.
Watson, J. P. N. (1975) Domestication and bone structure in sheep and goats. Journal of Archaeological Science 2, 375–383.
Weiner, S. (2010) Microarchaeology. Beyond the Visible Archaeological Record. Cambridge University Press, Cambridge.
Weiner, S. & Bar-Yosef, O. (1990) States of preservation of bones from prehistoric sites in the Near East: A survey. Journal of Archaeological Science 17, 187–196.
Weiner, S., Goldberg, P. & Bar-Yosef, O. (2002) Three-dimensional distribution of minerals in the sediments of Hayonim Cave, Israel: diagenetic processes and archaeological implications. Journal of Archaeological Science 29, 1289–1308.
Weiner, S. & Wagner, H. D. (1998) The material bone: structure-mechanical function relations. Annual Review of Materials Science 28, 271–298.
White, E. M. & Hannus, L. A. (1983) Chemical weathering of bone in archaeological soils. American Antiquity 48, 316–322.
Wilson, A. S., Dodson, H. I., Janaway, R. C. *et al.* (2007) Selective biodegradation in hair shafts derived from archaeological, forensic and experimental contexts. The British Journal of Dermatology 157, 450–457.
Wilson, A. S. & Tobin, D. J. (2010) Hair after death. In: Trüeb, R. & Tobin, D. (eds) Aging Hair. Springer-Verlag, Berlin, pp. 249–261.
Wolman, M. (1975) Polarized light microscopy as a tool of diagnostic pathology. A review. The Journal of Histochemistry and Cytochemistry 23, 21–50.